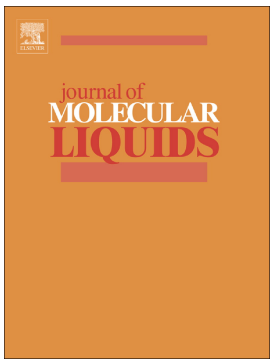

Biocompatible microemulsions for improved dermal delivery of sertaconazole nitrate: Phase behavior study and microstructure influence on drug biopharamaceutical properties

Natasa Bubic Pajić, Ines Nikolic, Evgenia Mitsou, Vassiliki Papadimitriou, Aristotelis Xenakis, Danijela Randjelovic, Vladimir Dobricic, Aleksandra Smitran, Nebojsa Cekic, Bojan Calija, Snezana Savic

PII:	S0167-7322(18)33575-X
DOI:	doi:10.1016/j.molliq.2018.10.002
Reference:	MOLLIQ 9747
To appear in:	*Journal of Molecular Liquids*
Received date:	11 July 2018
Revised date:	19 September 2018
Accepted date:	1 October 2018

Please cite this article as: Natasa Bubic Pajić, Ines Nikolic, Evgenia Mitsou, Vassiliki Papadimitriou, Aristotelis Xenakis, Danijela Randjelovic, Vladimir Dobricic, Aleksandra Smitran, Nebojsa Cekic, Bojan Calija, Snezana Savic , Biocompatible microemulsions for improved dermal delivery of sertaconazole nitrate: Phase behavior study and microstructure influence on drug biopharamaceutical properties. Molliq (2018), doi:10.1016/j.molliq.2018.10.002

Biocompatible microemulsions for improved dermal delivery of sertaconazole nitrate: phase behavior study and microstructure influence on drug biopharamaceutical properties

Natasa Bubic Pajić[a], Ines Nikolic[b], Evgenia Mitsou[c], Vassiliki Papadimitriou[c], Aristotelis Xenakis[c], Danijela Randjelovic[d], Vladimir Dobricic[e], Aleksandra Smitran[f], Nebojsa Cekic[g,h], Bojan Calija[b], Snezana Savic[b*]

[a] Department of Pharmaceutical Technology and Cosmetology, Faculty of Medicine, University of Banja Luka, Save Mrkalja 14, 78000 Banja Luka, Bosnia and Herzegovina, natasa.bubic.pajic@med.unibl.org

[b] Department of Pharmaceutical Technology and Cosmetology, Faculty of Pharmacy, University of Belgrade, Vojvode Stepe 450, 11221 Belgrade, Serbia, snezana.savic@pharmacy.bg.ac.rs

[c] Institute for Biology, Medicinal Chemistry and Biotechnology, National Hellenic Research Foundation, Athens, Greece, vpapa@eie.gr

[d] ICTM – Institute of Microelectronic Technologies, University of Belgrade, Njegoševa 12, Belgrade, Serbia, danijela@nanosys.ihtm.bg.ac.rs

[e] Department of Pharmaceutical Chemistry, Faculty of Pharmacy, University of Belgrade, Vojvode Stepe 450, Belgrade, Serbia, vladimir@pharmacy.bg.ac.rs

[f] Department of Microbiology, Faculty of Medicine, University of Banja Luka, Save Mrkalja 14, 78000 Banja Luka, Bosnia and Herzegovina, aleksandra.smitran@med.unibl.org

[g] Faculty of Technology, University of Niš, 16000 Leskovac, Serbia, nesafarm@gmail.com

[h] DCP Hemigal, 16000 Leskovac, Serbia

* Corresponding author: Dr Snežana Savić, Department of Pharmaceutical Technology and Cosmetology, Faculty of Pharmacy, University of Belgrade, Vojvode Stepe 450, 11221 Belgrade, Serbia

Tel.:+381-11-3951366 Fax: +381-11-3972840

E-mail address: snezana.savic@pharmacy.bg.ac.rs (S. Savić)

Abstract

The aim of this study was development of biocompatible topical microemulsions (MEs) for incorporation and improved dermal delivery of sertaconazole nitrate (SN). For this purpose, phase behavior and microstructure of pseudo-ternary ~~surfactant~~ glycereth-7-caprylate/caprate (Emanon EV-E, EV)/cosurfactant/ Capryol™ 90/ water systems were investigated. Furhermore, the influence of these properties on the drug skin delivery was also assessed. ~~Glycereth-7-caprylate/caprate (Emanon EV-E, EV) was used as surfactant, whereas Transcutol® P, ethanol, isopropyl alcohol, glycerol and propylene glycol were evaluated as cosurfactants.~~ Expansion of ~~microemulsion~~ ME single-phase regions with the use of short chain alcohols was a consequence of the more fluid interface when compared to other investigated systems, which was confirmed by electron paramagnetic resonance spectroscopy – EPR ~~(obtained rotational correlation time values ranged from 1.55 ns to 3.83 ns)~~. ~~Bicontinuous to inverted bicontinuous inner microstructure of the selected vehicles with different qualitative (and quantitative) composition was suggested by comprehensive physicochemical characterization.~~ The chosen bicontinuous to inverted bicontinuous formulations were assessed against the ~~microemulsion~~ ME based on polysorbate 80 as referent sample. Despite incorporation of SN within the selected formulations induced similar alternations in electrical conductivity, viscosity and pH values~~. Depending on formulation composition~~, obtained EPR spectra suggested different SN localization: within the oil phase (for most of the EV based formulations), or interacting with the interface (polysorbate 80 based formulation). Due to higher i*n vitro* drug release (12.24% - 18.53%), *ex vivo* SN penetration into porcine ear skin (dermal retention Enhancement Ratio (ER_D) ranged from 2.66 to 4.25) and pronounced antifungal activity, the chosen MEs represent promising vehicles for dermal delivery of SN in treatment of cutaneous fungal infections. ~~The percentage of the SN~~

released from MEs was in range of 12.24% - 18.53%, which was significantly higher in 4 out of 5 investigated MEs in comparison with the commercial product (10.33%). Similar findings were revealed in *ex vivo* SN penetration experiment into the porcine ear skin - Dermal Retention Enhancement Ratio (ER_D) ranged from 2.66 to 4.25. The biopharmaceutical and skin performance differences obtained with different formulations were possible to be explained on the basis of their physicochemical characteristics. Due to the higher SN penetration into the skin and pronounced antifungal activity, the chosen MEs represent promising vehicles for dermal delivery of SN in treatment of cutaneous fungal infections.

Keywords: glycereth-7-caprylate/caprate, sertaconazole nitrate, microemulsion, electron paramagnetic resonance spectroscopy, in vitro release, penetration

Abbreviations[1]

Abbreviations: microemulsion (ME)**,** Emanon EV-E (EV), Capryol^{TM} 90 (C90), polysorbate 80 (P80), surfactant-cosurfactant (S-CoS), dermal delivery enhancement ratio (ER_D)

1. Introduction

The major obstacle in the conventional topical treatment of deep fungal skin infections, where therapeutic effects should be restricted to the affected area and systemic incrimination reduced, is the uppermost layer of the skin, the *stratum corneum*. Namely, the effectiveness of a topically applied antifungal agent is directly related to its ability to reach at least the viable epidermis [1]. But, the latter one is mostly dependent on the drug physicochemical properties and the vehicle used for its administration [2]. Considering that many antifungals are poorly soluble and have low skin permeability [1], development of a suitable formulation, capable of drug delivering to the target skin layer, is highly challenging. As an imidazole derivative which inhibits the synthesis of ergosterol, sertaconazole nitrate (SN) is indicated for the treatment of dermatophyte infections (tinea corporis, tinea cruris, tinea manus, tinea barbae and tinea pedis), cutaneous candidiasis, vaginal candidiasis, pityriasis versicolor and seborroeic dermatitis of the scalp [3]. However, SN has unfavorable physicochemical properties regarding topical administration, i.e. poor aqueous solubility with high partition coefficient (logP = 6.2) [1], hindering its practical use and leading to low dermal bioavailability. In order to deliver SN into deeper skin layers, different strategies and modern drug carriers have been recently proposed [4-10]. Among them, microemulsions (MEs) seem to be particularly appealing due to their numerous advantages. As spontaneously and easily prepared, optically isotropic, transparent, low viscous dispersions of oil, water, surfactant and often cosurfactant, MEs are thermodynamically stable and offer well established drug skin permeation enhancement effect. Although the exact mechanism responsible

for enhanced drug permeation has not been completely elucidated, several possibilities are suggested: higher solubilization capacity coupled with high concentration gradient, increased drug thermodynamic activity, relatively high surfactant/cosurfactant content, as well as some specific properties related to the inner structure of this nanocarrier [11-14]. However, there is a constraint on topical MEs formation arising from excipients acceptability and high amounts of surfactants associated with potential skin irritating effect. Therefore, a large number of studies involved nonionic, biodegradable, nontoxic surfactants, which are either synthetic or of natural origin. Among synthetic tensides used to stabilize MEs, polyethoxylated surfactants, such as polysorbates, seem to be most frequently used due to their minimal toxicity reported [15]. Although a great number of investigations have dealt with the use of polyoxyethylene (glycerol) fatty acid esters as stabilizers in ME systems [2], to the best of our knowledge, none of these formulations have been based on glycereth-7-caprylate/caprate (Emanon EV-E, EV). Hence, in order to investigate deeper the EV's ability to form stable MEs, we extended our previous study [16] and tested the emulsification power and phase behavior of the aforementioned surfactant in the presence of several usually employed cosurfactants/cosolvents (Transcutol® P, ethanol, isopropyl alcohol, propylene glycol, glycerol). Based on the hypothesis that structural differences in the used cosurfactants may result in distinct nanostructures with different physicochemical properties, skin tolerability, as well as the capability for dermal drug delivery [12, 13, 17], we investigated physicochemical and biopharmaceutical characteristics of several placebo and SN-loaded MEs obtained with EV in combination with different cosurfactants, comparing them mutually. A comparison was also made related to the ME stabilized with polysorbate 80 (P80), which served as the referent ME carrier, as well as to the commercially available drug product (SN-loaded cream sample). Hence, the main goal was to produce stable topical ME formulations

with enhanced skin retention without compromising antifungal activity of the drug. However, despite the extensive studies, a real therapeutic efficacy of ME formulation can hardly be predicted. Therefore, an attempt to correlate physicochemical characteristics of the investigated vehicles to their biopharmaceutical performances was also made. In this course, samples were subjected to the conductivity studies, differential scanning calorimetry (DSC), atomic force microscopy (AFM) and electron paramagnetic resonance (EPR) analysis coupled with the one year storage-stability study and *in vitro* SN release and porcine ear skin permeation/penetration assessment followed finally by *in vitro* antifungal activity evaluation.

2. Materials and methods

2.1. Materials

SN and SN reference standard were purchased from Shanghai Pengteng Fine Chemical (Shanghai, China) and Sigma Aldrich (Steinheim, Germany), respectively. EV was kind donation from Kao Chemicals (Barbera del Valles, Spain), whereas propylene glycol monocaprylate (Capryol™ 90, C90) and highly purified diethylene glycol monoethyl ether (Transcutol® P) were kindly gifted from Gattefosse (Lyon, France). Propylene glycol was supplied by Kemig (Zagreb, Croatia), P80 by Sigma–Aldrich Laborchemikalien GmbH (Seelze, Germany), ethanol by ZorkaPharm (Sabac, Serbia), isopropyl alcohol and glycerol by Lach-Ner (Neratovice, Czech Republic). 5-doxyl stearic acid (5-DSA) was the product of Sigma-Aldrich, (Steinheim, Germany). HPLC grade water was obtained with a GenPure apparatus (TKA water purification system, Niederelbert, Germany). Mycosert® cream was provided by pharmacy store. All other chemicals were of pharmaceutical or HPLC grade and were used as received without purification.

2.2. Construction of pseudo-ternary phase diagrams and preparation of MEs

Phase behavior of systems comprising of oil (C90), surfactant-cosurfactant mixture (S-CoS) and water was explored by construction of pseudo-ternary phase diagrams, using water titration method. Different weight ratios of C90 and S-CoS mixture ranging from 1:9 to 9:1 (*w/w*) were prepared and water was gradually added in a drop wise manner (Vortex Mixer, Velp Scientifica, Italy). The S-CoS mass ratio (K_m) was kept at 1. Boundaries of ME area were determined according to the largest amount of water incorporated in homogenous, single-phase, low viscous and transparent ME samples. The appearance of opalescence or turbidity was considered as an indicator of phase separation. Further, selected MEs were prepared by mixing the oil with S-CoS for 15 min at magnetic stirrer (Falc, Italy). Then the proper amount of water was added with gently magnetic stirring for another 30 min. SN was dissolved in the pre-weighted ME vehicles under continuous mixing at magnetic stirrer for 2h followed by ultrasonication for 15 min to give a final concentration of 2% (*w/w*).

2.3. Microemulsion characterization

2.3.1. Polarized light microscopy

Transparent placebo and drug loaded ME samples were submitted to polarization microscopy (Olympus BX51-P, Olympus Corporation, Tokyo, Japan) in order to confirm their isotropy and complete solubilization of SN in final vehicles.

2.3.2. Electrical conductivity

Electrical conductivity measurements were carried out at room temperature using SensION EC71 instrument (Hach Company, Loveland, Colorado) with a cell constant of 1.0 cm^{-1}. To

evaluate the MEs' inner structure water was added gradually into the initial mixture of S-CoS and oil, and conductivity of obtained samples was checked after the equilibrium was attained. Bearing in mind that phase behavior of nonionic tensides and thus ME nanostructure can be altered in the presence of electrolytes due to the modification of ionic strength of water phase and its chemical potential [18, 19], this study was performed without electrolyte addition. Measurements were made in triplicate for each sample.

2.3.3. Rheological measurements

The rheological properties of the prepared ME formulations was assessed on DV-III ULTRA Programmable Rheometer & Rheocalc software v.4.3 (Brookfield Engineering Laboratories, Middlesboro USA), coupled with cone and plate measuring device at 20 ± 1°C. Measurements were performed in triplicate at shear rates in range of 75-750 s^{-1}, for both, up and down curves.

2.3.4. pH analysis

The pH values of MEs were measured using pH meter (HI9321, Hanna Instruments, Portugal). Experiments were performed in triplicate for each sample.

2.3.5. Differential scanning calorimetry (DSC) measurements

In order to obtain further insight into the microstructure and type of prepared MEs, the physical state of water in nonionic MEs was investigated by using low-temperature DSC (Mettler Toledo DSC 1, STAR^e System (Mettler Toledo AG, Analytical, Switzerland)). DSC cooling curves were conducted with approximately 10 mg of ME samples weighted into aluminum pans and quickly sealed to prevent water evaporation from the samples. Simultaneously, a reference was an empty

hermetically sealed pan. Placebo ME formulations were cooled from 25°C to –60°C (cooling rate: 5°C/min) under constant nitrogen flow (50 ml/min).

2.3.6. Atomic force microscopy (AFM)

Surface morphology of the chosen placebo ME was observed using atomic force microscopy (NTEGRA prima AFM, NT-MDT, Moscow, Russia) operating in intermittent-contact AFM mode in air and NT-MDT NSGO1 silicon cantilevers (N-type, Antimony doped, Au reflective coating). For more details, please consult the supplementary material section. ~~For this purpose, a drop (10 µL) of the sample was directly deposited onto a small, circular mica substrate (Highest Grade V1 AFM Mica Discs; Ted Pella Inc., Redding, California) and dried in desiccator for 48 h to remove excess water. During the measurements, experimental conditions were set as follows: nominal force constant 5.1 N/m, resonance frequency 87–230 kHz, driving frequency 148 kHz, and line scanning frequency 1 Hz. For the investigated samples, two types of images, topography and "error signal" AFM images, were taken and later analyzed using the software Image Analysis 2.2.0 (NT-MDT, Moscow, Russia).~~

2.3.7. Electron paramagnetic resonance spectroscopy (EPR)

EPR using the spin-probing technique was employed in order to study microenvironment properties of the interface comprising of S-CoS monolayer and to investigate drug interactions with the interface of selected MEs on molecular level [20, 21]. The spin probe having capability to reflect ordering and dynamics of the interfacial film at different depths was used: the doxyl free radical, 5-doxyl stearic acid [5-(1-oxyl-2,2-dimethyl-oxazolidin) stearic acid, 5-DSA). As a fatty acid, 5-DSA has an amphiphilic nature deriving from the presence of a polar head group (-COOH) and a hydrophobic moiety. Due to the structure of 5-DSA and especially of the location

of the nitroxide paramagnetic ring (doxyl group) at the 5th carbon atom of the hydrocarbon chain, the unpaired electron is located closer to the polar head of the fatty acid and consequently closer to the S-CoS polar head group area [22, 23]. 5-DSA was added in the systems as described previously [20]. For detailed description of the experimental procedure and analysis of the experimental results, please consult the supplementary material section. ~~Briefly, to obtain the desired concentration of the spin probe in the MEs, 1 ml of each ME was added to a tube into which the appropriate amount of the spin probe had been deposited previously. More specifically, 15 μl of an ethanolic stock solution of 5-DSA (7.8×10^{-3}M) were transferred in the tube and the solvent was allowed to evaporate at room temperature. The samples remained overnight in a water bath (25°C). Final concentration of 5-DSA in the MEs was 0.117 mM.~~

~~EPR spectra were recorded at constant room temperature (25°C), using a Bruker EMX EPR spectrometer operating at the X-Ban, USA. Experiments were conducted with the use of a WG-813-Q Wilmad (Buena, NJ) Suprasil flat cell. Typical instrument settings were: Center field: 0.349 T, scan range: 0.01T, gain: 5.64×10^{3}, time constant: 5.12 ms, modulation amplitude: 0.4 mT and frequency: 9.78 GHz. Data collection and analysis were performed using the BrukerWinEPR acquisition and processing program.~~

~~Experimental results were analyzed in terms of rotational correlation time (τ_R), order parameter (S) and isotropic hyperfine splitting constant (α'_o). The rotational correlation time, τ_R, of the spin probes was calculated from the EPR spectra according to the following equation [24]:~~

$$\tau_R = (6 \times 10^{-10})\left[(h_0/h_{+1})^{1/2} + (h_0/h_{-1})^{1/2} - 2\right]\Delta H_0 \, (s) \quad (1)$$

~~where h_{+1}, h_0, and h_{-1} represent the amplitudes of the three hyperfine lines respectively and ΔH_0 is the width of the central line. The above mentioned relationship is applicable in the fast~~

motion region, i.e. for τ_R in the range $10^{-11} < \tau_R < 3 \times 10^{-9}$ s, where spin probes are sensitive to small changes in their microenvironment. Therefore, the variation of the τ_R values reflects the restrictions imposed on its motion from the specific microenvironment. For the slow motion region ($\tau_R > 3 \times 10^{-9}$s) the rotational correlation time, τ_R, is calculated with the use of computer simulations assuming average rotational correlation times.

From the spectral characteristics, two more parameters were calculated: the order parameter, *S*, and the isotropic hyperfine splitting constant, α'_o. The order parameter (S) describes the orientational order of spin probe depending on its arrangement in a supramolecular assembly. *S* varies from $S = 1.0$ for perfectly ordered membranes to $S = 0$ for the completely random state. From EPR spectra, *S* is calculated using the following relationship [21, 22]:

$$S = (A_{\shortparallel} - A_{\perp})/[A_{zz} - 1/2(A_{xx} + A_{yy})](\alpha'_0/\alpha_0) \quad (2)$$

where A_{xx}, A_{yy}, and A_{zz} are the single-crystal values of the spin probe indicative for doxyl derivatives and are equal to 0.63, 0.58 and 3.36 mT, respectively. The ratio α'_0/α_0 is the polarity correction factor (hyperfine splitting constants), where α_0 is $\alpha_0 = (A_{yy} + A_{xx} + A_{zz})/3$ and α'_0 is the isotropic hyperfine splitting constant for the spin probe in the membrane and is defined as

$\alpha'_0 = (A_{\shortparallel} + A_{\perp})/3$. $A_{\shortparallel}$ corresponds to the half distance of the outer maximum hyperfine splitting (A_{max}), while $A_{\perp}$ is defined as:

$$A_{\perp} = A_{min} + 1.4(1 - S^{app}) \quad (3)$$

and

$$S^{app} = (A_{max} - A_{min})/[A_{zz} - (1/2)(A_{xx} + A_{yy})] \quad (4)$$

where A_{min} is equal to the half-distance of the inner minimum hyperfine splitting.

~~The hyperfine splitting constant, reflecting the polarity in the environment of the doxyl paramagnetic ring, can be also calculated directly from the EPR spectrum. α_0' value is taken as the distance between the first and the second line (peak) of the first derivate of the EPR spectrum. The α_0' value is sensitive to the polarity of the environment of the spin probe and is increased when the polarity of the medium is increased.~~

2.3.9. Saturation solubility of SN in MEs

The saturation solubility of the drug in chosen ME formulations was determined by shake flask method. An excess drug amount was added in the selected formulation (5 mL) and stirred continuously (IKA® KS 260 basic shaker, IKA® Werke GmbH & Company KG Staufen, Germany) for 72 h at mixing rate of 300 rpm at room temperature to reach equilibrium. After removal of undissolved drug by centrifugation (3000 rpm for 30 minutes (Centrifuge Rotofix 32 A, Hettich, Tuttlingen, Germany)), the supernatant was filtered through 0.22 µm membrane filter (Chromafil® Xtra PTFE-20/25, Macherey-Nagel, Düren, Germany) and concentration of the drug was determined by using high performance liquid chromatography methodology (HPLC).

2.4. Stability study

Physical and chemical stability of SN loaded MEs and of their blank counterparts stored at the room temperature (20 ± 3 °C) was assessed at different time points during a year of storage.

2.5. In vitro *release of sertaconazole nitrate*

In vitro drug release profiles of The selected SN loaded ME formulations (Table 1) and referent cream were assessed utilizing vertical diffusion (Franz) cells (Gauer Glas, D-Püttlingen, Germany) according to USP general monograph for semisolid drug products [24]. Each receptor

chamber (effective diffusion area: 2.01 cm^2) was filled with precise volume (12 mL) of degassed preheated (32 °C) mixture of ethanol and water (50:50 v/v) and continuously stirred with a magnetic stirrer at 500 rpm. Previously activated dialysis membranes (with a pore size of 2.4 nm and molecular weight cut-off 12000) were carefully mounted between donor and receptor compartments. The investigated MEs (1 g) were placed on the membranes, spread to cover entire membrane, and then covered with occlusive Parafilm™ to prevent any evaporation. The temperature of diffusion cells was maintained at 32 °C throughout the experiment using circulating water bath. Aliquots (600 µL) were withdrawn and replaced with an equal volume of fresh pre-warmed medium after 30 min, 1 h, 2 h, 3 h, 4 h, 6 h and 8 h of samples application. The withdrawn samples were analyzed for SN concentration using HPLC method. The results are expressed as the cumulative amount of drug released per unit area (µg/cm^2) plotted versus time (t), allowing the determination of *in vitro* transmembrane flux for each investigated ME sample. In order to compare the obtained drug release profiles, statistical and model-dependent approaches were proposed.

2.6. Ex vivo *penetration and permeation assessment*

Ex vivo penetration and permeation test was conducted using porcine ears obtained from the local abattoir~~,~~. Immediately after slaughter, the porcine ears were washed under cold running water, blotted dry with a soft tissue and stored at −20 °C. Briefly, on the day of the experiment, they ~~porcine ears~~ were thawed at room temperature. In order to remove visible hairs from the skin, a hair clipper was used. Afterwards, subcutaneous fat was removed from the skin with a surgical blade and the skin pieces, having a diameter of 25 mm and suitable for permeation studies, were punched. The obtained skin sections were checked for any physical damage and soaked in a mixture of ethanol and water (50:50 v/v) for 1h to equilibrate and rehydrate. Then the

porcine ear skin pieces were clamped between the donor and receptor compartments of modified Franz diffusion cells (Gauer Glas, D-Püttlingen, Germany) with 2.01 cm^2 permeation area and 12 mL receptor cell volume. The *stratum corneum* layer was positioned on the assembly facing the donor compartment. The investigated formulations (1 g) were carefully applied to the skin surface. Experiments were carried out in triplicate, at 32 °C, using ethanolic water (50:50 v/v) as receptor medium, stirred constantly at 500 rpm. Samples (600 µL) were withdrawn at appropriate intervals (2 h, 4 h ,6 h, 8 h and 24 h) over 24 h and immediately replaced with the same volume of freshly prepared medium kept at the same temperature. In order to determine the drug permeated, the aliquots were submitted to HPLC analysis. Finally, at the end of the permeation test, the skin samples were removed, wiped clean three times with PBS (pH = 7.4) to remove excess formulations and cut into small pieces. Then, the skin pieces were transferred to capped volumetric flasks filled with 5 ml of methanol and subjected to SN extraction by mixing on a laboratory shaker for 24 h (IKA® Werke GmbH & Company KG Staufen, Germany). Afterwards the content of flasks was sonicated (Sonorex RK 120H, Bandelin, Berlin, Germany) for 30 min in order to ensure maximum extraction of the drug and then centrifuged at 4000 rpm for 20 min (Centrifuge MPW-56; MPW Med. Instruments, Warszawa, Poland). The obtained supernatants were filtered (membrane filter 0.45 µm) and HPLC analysis was conducted in order to determine SN concentration.

2.7. In vitro *antifungal activity*

The selected ME formulations along with Mycosert® cream were assayed for their antifungal activity against the fungal strain *Candida albicans*. In order to evaluate antifungal efficacy of the tested samples the cup plate diffusion method was employed. *Candida albicans* was grown on solidified Sabauroud's agar medium poured into sterilized Petri dishes under laminar air flow.

The cups were cut using sterilized cork borer, while MEs and cream were accurately filled into different cups with the aid of sterilized syringes. The Petri dishes were then covered with lids and incubated at 37±0.1 °C for 24 h to allow fungal growth. The antifungal activity was expressed as zone of inhibition (mm) of fungal growth surrounding the formulations. All determinations were made in triplicate for each sample.

2.8. Drug analysis

The drug quantification was carried out with the use of the established HPLC method [25]. For more detail on the method, please consult the supplementary material section. ~~The HPLC analysis was performed on Dionex Ultimate 3000 system (Thermo Fisher Scientific, Dreieich, Germany) equipped with Dionex Ultimate 3000 quaternary pump, autosampler and DAD detector. The column chosen was Zorbax Eclipse XDB-C18 (150 mm × 4.6 mm, 5 µm particle size). The mobile phase consisted of methanol and 0.2% formic acid (70:30, v/v). The column temperature was adjusted to 30ºC and the flow rate was 1 ml/min. The detection was performed at 260 nm.~~

2.9. Data analysis

All the tests were performed in 3-6 replicates and data were expressed as the average value ± SD. The data were statistically analyzed by one-way analysis of variance (ANOVA), with statistical significance set at $p < 0.05$, which was considered as significant with 95% confidence intervals. Statistical analysis was performed using Microsoft Excel software package.

3. Results and discussion

3.1. Pseudo-ternary phase diagrams

According to the manufacturer's specification, EV is a vegetable-based, eco-friendly nonionic surfactant, being both biodegradable and with low toxicity. It is generally used for hair and skin care applications and characterized with high content of monoester and a very high value of HLB (HLB ~ 17) as well. However, in order to develop pharmaceutically applicable ME systems based on novel, scarcely characterized surfactants such as EV, phase behavior studies are prerequisite. Indeed, the recognition of the phase behavior and water solubilization capacity of nonionic surfactants in the system are considered as key factors for formation of MEs as potential drug delivery systems [26]. As the mutual miscibility of the oil and surfactant and the consequent oil emulsification are greater if the oil and surfactant chain length are similar [27], propylene glycol monocaprylate (C90) was selected as the oil phase. Moreover, C90 and EV as well showed a high potential to dissolve the drug [16]. However, taking into account that a single surfactant is usually not sufficient to form a stable ME, five distinct cosurfactants were varied (Transcutol® P, ethanol, isopropyl alcohol, propylene glycol and glycerol) in order to assess their influence on the rigidity/flexibility of the interfacial film, and hence, on the single-phase area. Figure 1a shows different pseudo-ternary phase diagrams obtained with EV as surfactant, Transcutol® P, ethanol, isopropyl alcohol or propylene glycol as a cosurfactant, C90 as the oil and double distilled water. It should be pointed out that EV is able to produce MEs in the absence of cosurfactants only with oil:S-CoS ratios 9:1 and 8:2 (data not shown). Under these conditions, maximum water incorporation along the dilution line 8:2 was 16.67% (w/w), while the initial mixture oil:S-CoS equals 9:1 was fully dilutable. However, the usage of aforementioned cosurfactants resulted in widening of the single phase area obtained with the surfactant alone. As expected, the maximum water incorporation was reached at very low oil concentrations, reducing sharply as the oil content became higher. Also, outside ME areas,

coarse emulsions were formed. Comparing the effects of the tested cosurfactants, it could be noticed that the smallest ME area was obtained when propylene glycol was used as cosurfactant. Interestingly, EV in a combination with glycerol had no efficacy in formation of ME systems. The largest area of MEs' existence was obtained with isopropyl alcohol because it was probably the best distributed between the hydrocarbon chains of oil and surfactant increasing the interfacial flexibility and making the interface less sensitive to water dilution. Hence, ME area increased as the chain length of alcohol increased from ethanol to isopropyl alcohol, while the increase of hydroxyl groups number from isopropyl alcohol to propylene glycol reduced the size of ME zone such as glycerol completely abolished the single phase area that was in line with previously reported findings obtained with polysorbate 80 and lecithin [20, 28, 29]. Introduction of cosurfactants into oil/water/surfactant system leads to further reduction of interfacial tension and affects surfactant packing, allowing the interfacial film to be sufficiently flexible to take up adequate curvatures necessary for ME formation over a wide range of composition [28-31]. Depending on their polarity/amphiphilicity, the low molecular weight cosurfactants are distributed between the oil and water, affecting the hydrophilicity/lipophilicity balance [30]. In fact, the size of ME areas obtained with cosurfactants used in this study can be correlated with their partition coefficients as a measure of their polarities, which in turn determine the solubilization locus of cosurfactants in ME systems. Analyzing the obtained results, it seems that a cosurfactant's ability to penetrate into the amphiphilic film decreases with increasing polarity. Indeed, the most polar cosurfactant (glycerol, logP = -1.76) produced no MEs, whereas the widest ME area was obtained with the least polar one (isopropyl alcohol, logP = 0.05). Accordingly, less polar cosurfactant, such as isopropyl alcohol, inserts itself among the surfactant molecules with its hydroxyl group facing water. This made the interface less sensitive

to water dilution and increased the mutual miscibility of oil and water. On the other hand, propylene glycol and glycerol having two and three free hydroxyl groups, respectively, probably migrated from the interface and were mostly located in water phase. As a result, the amphiphiles concentration at the interface was reduced by water addition, destabilizing the ME system. Further, despite both used monohydric alcohols have one hydroxyl group, ethanol produced narrower single phase area than isopropyl alcohol, which can be also attributed to higher polarity of ethanol (logP = -0.31). Finally, the decrease of the total ME area in the case of Transcutol® P (logP = -0.54) when compared to short chain alcohols may be also attributed to its higher polarity. On the other hand, Transcutol® P produced wider ME area than propylene glycol because propylene glycol (logP = -0.92) is too soluble in the aqueous phase and thus less effective as cosurfactant.

These results undoubtedly demonstrate that EV, as nonionic surfactant with high HLB value (~17), can be included to the list of polyethoxylated surfactants capable of forming ME systems over wide range of costituents. Qualitative and quantitative compositions of MEs determine their inner structure, physicochemical characteristics, droplet shape and size and affect the placement and the fate of a particular solute such as drug molecule [11, 12, 32]. When it comes to dermal drug delivery, the drug has to liberate from the vehicle in order to penetrate into the skin. The liberation process is dependent on the hosting environment properties, such as physicochemical characteristics and dynamics. Cohen-Avrahami and coworkers [33] have recently demonstrated that the release of sodium diclofenac was significantly greater from the cubic mesophase than from the lamellar system due to the different drug interactions with the respective interfaces. Also, it has been already reported that dermal delivery of the hydrophobic antifungal drug is affected by microstructure of MEs [12]. However, the possibility of producing MEs with diverse

inner structures cannot be completely anticipated from the obtained phase diagrams. Therefore, structural characterization was further conducted.

3.2. Structural characterization and selection of samples

In order to assess microstructural changes upon dilution with water, electrical conductivity (κ) was measured and plotted as a function of water content (Φ_w). Despite slightly lower water solubilization along the dilution line S-CoS:oil=8:2 than along the line 9:1, we selected the dilution line 8:2 for further structural characterization with the intention to reduce surfactant content in final formulations, increasing their biocompatibility [19]. In addition, the maximum drug penetration enhancement is usually not obtained if the amount of surfactant in formulation was the highest [2, 13, 32].

Figure 1b shows changes of electrical conductivity (κ) of the investigated systems with gradual increase of water, until maximum water was added within the single-phase ME areas. As can be noticed, the investigated systems containing less than 10% of water had low electrical conductivity values. With further addition of water up to maximal water solubilization, conductivity increased to the maximal values. This can be explained with the progressive increase in hydration of ethylene oxide moieties of EV, rendering a better conducting entity. Namely, below a critical value of Φ_w water molecules are isolated from each other because being embedded in the non-conducting continuous oil phase, contributing very little to the electrical conductivity [14, 34]. As water if further added, the number of non-interacting droplets is greater, reaching its critical value and leading to interlinking and clustering of the droplets, which reflects as a pronounced rise of conductivity. However, the analysis of the obtained conductivity plots revealed no typical percolative behavior, at least for MEs based on ethanol,

isopropyl alcohol and propylene glycol. Therefore, the exact points of microstructure transition from water-in-oil (w/o)) to oil-in-water (o/w) MEs through emergence of bicontinuous systems were not observable. In order to assess the validity of percolation theory and elucidate the percolation threshold, the first derivative of κ ($d\log(\kappa)/d\Phi_w$) was plotted as a function of Φ_w. The *first derivative approach* allows the determination of a percolation threshold from a maximum in the curve [35]. Hence, quantity of $d\log(\kappa)/d\Phi_w$ was evaluated for each system and presented in Figure 1b. In accordance with our previous assumptions, phase transitions occurred at very low water contents in each of the studied systems. Actually, considering ethanol based system, it is possible that percolation was achieved even in sample with no water added. This can be explained on the basis of certain residual amount of water present in ethanol (96% v/v), used in this study. Therefore, the sample without externally added water may contain *per se* enough water to produce bicontinuous structure instantly. Since the maximum of the curve can be noticed when fraction of water added equals zero, it seems that phase transition from w/o to bicontinuous microstructure had been already occurred or it was ending in this point. Similar lack of percolation threshold point was noticed in lecithin based MEs costabilized with ethanol [20].

However, in other investigated ME systems, the presence of percolative behavior was confirmed with observable sharply peaked maximum values of the plots showing $d\log(\kappa)/d\Phi_w$ versus Φ_w (Figure 1b). The obtained maximal values were at 2, 2.5 and 3%, for systems containing propylene glycol, Transcutol® P and isopropyl alcohol, respectively. As revealed by phase behavior studies, more polar cosurfactants are less solubilized in the surfactant interfacial film. Such cosurfactant location within the system reduced the strength of forces that stabilize the

interface and enhanced interdroplet interactions. As a result, percolation threshold was more easily achieved.

Taking into account the results obtained by using electrical conductivity measurements, EV was capable to produce w/o and/or bicontinuous MEs along the selected dilution line (8:2). Because the second slope on the respective curves implying inversion from bicontinuous to o/w MEs is not visible, fully developed water continuous systems were not anticipated. Bearing in mind that bicontinuous MEs have several benefits over globular type of MEs, i.e. higher amphiphilic character, greater fluctuating interface, a lower interfacial tension and improved solubilizing properties [36], we selected vehicles with presumed (inverted) bicontinuous microstructure as carriers for SN. In addition, o/w and bicontinuous MEs are generally considered as carriers which enhance penetration/permeation of hydrophobic drugs much more than oil continuous microemulsions [2, 12, 32]. Hence, the selection was done based on the ability of the sample with minimum surfactant and maximum water content of solubilizing the drug therapeutic concentration (2% w/w) and satisfying preliminary stability. The composition of the selected formulations and SN solubility within these samples are given in Table 1. With the exception of ME with propylene glycol, such a selection allowed us to elaborate the influence of cosurfactant type on MEs properties. However, the formulation with propylene glycol contained less water than other samples. Although SN could be solubilized within this sample, the ME with 30% of water phase was near the border of the respective single phase area and it was excluded due to potential stability issues. In addition, quantitatively the same ME based on P80 as commonly employed surfactant in ME formulation was used. Transcutol® P was chosen as cosurfactant in the referent sample because SN has the highest solubility in this cosurfactant [16].

In order to further check the results obtained with electrical conductivity measurements and confirm the internal microstructure of the selected vehicles, DSC in cooling mode was carried out. Namely, by analyzing samples with DSC, a differentiation between different physical states of water within dispersed systems can be accomplished. This is based on the fact that bound (immobilized internal or interfacial) water has freezing point at subzero temperatures, while free bulk water molecules, located far from the interfacial layer and thus having high mobility, freeze in the vicinity of zero degrees [14, 37]. Cooling curves of the selected vehicles (Table 1), in spite of having 25-30% of water, resulted in no freezing peaks (Figure 2), suggesting their oil-continuous inner structure characterized with non-freezable aqueous phase [27, 38]. However, according to Podlogar et al [38] and Goebel et al [37], the absence of an exothermic water peak could be explained with the strong interactions between S-CoS molecules with water, which shifted freezing of water towards lower temperatures. Taking into account that the chosen samples contain at least 28% (*w/w*) of surfactant and 28% (*w/w*) of cosurfactant, the hydration of the hydroxyl groups of surfactant and cosurfactants cannot be neglected. Moreover, having in mind C90's surface active properties and one free hydroxyl group, the interactions between water and oil can be also suggested. Consequently, water freezing point moved towards lower temperatures, which were probably out of the detected range. Therefore, strong interactions in the investigated systems were proposed as the main reasons for the disagreement between the results obtained with electrical conductivity and DSC.

On the other hand, AFM as a rarely used direct technique for ME characterization supported the assumptions revealed by using indirect methods. The AFM images – error signal and 3D topography of the chosen ME-EVI are illustrated in Figure 3. As can be seen from the micrographs, AFM detected the structure of ME-EVI sample predominantly characterized with

lack of long-range order and fluctuating interface separating mutually intertwined oil and water domains. However, non-uniform rare oil droplets can be also observed, implying the onset of system inversion from bicontinuous to water-continuous MEs. High electrical conductivity value of ME-EVI argues in favor of this claim. Additionally, it is important to note that MEs, as highly dynamic systems, spontaneously and continuously undergo fluctuations including phase transitions and changes in droplet size [13]. Furthermore, it should be also underlined that the difficulty was found in obtaining high quality images due to problems with sample preparation resulted in incomplete removal of excess liquid. Briefly, the tested samples must be attached to a surface in order to prevent movement, sample's damage and modifications, which could potentially induce the microstructure and surface phenomena changes. Nevertheless, the obtained AFM results enabled the differentiation of the MEs from the geometrically ordered lamellar liquid crystals structures with higher viscosity and pseudo-plastic flow behavior [27, 34].

3.3. Physicochemical characterization of the selected MEs

Considering that even slight changes in composition of MEs reflect on their physicochemical characteristics and consequently on drug biopharmaceutical properties, comprehensive physicochemical characterization was carried out in order to gain insight into drug-vehicle interactions and factors involved in drug release and penetration. Physicochemical properties of the selected MEs are presented in Table 2 and Figure 4.

Polarization microscopy results were in high agreement with AFM microscopy, suggesting the lack of liquid crystalline structures for placebo samples as well as SN-loaded MEs. pH values of the tested placebo samples were in range of 4.13-7.47. Solubilization of SN within the MEs caused significant decrease of pH (3.67-4.65), but still acceptable for intended dermal

application. The dramatic decrement of pH values was attributed to the presence of strongly acidic nitrate anions in aqueous phase. EV-based samples characterized with slightly distinct pH values, whereas the reference sample stabilized with P80 had significantly lower pH.

Electrical conductivity is considered to be a structure-sensitive property of a ME system. The rank order of conductivity values of EV based MEs (ethanol > isopropyl alcohol > Transcutol® P > propylene glycol) may be also related to the polarity and the location of each cosurfactant in the respective systems. For example, propylene glycol has the highest hydrophilicity and most likely it migrated out of the interface into the water phase to a greater extent than the other cosurfactants. Consequently, hydration of its hydroxyl groups took place, restricting the mobility of water molecules and hence the electrical conductivity values decreased. Due to the presence of one hydroxyl group in their structures, ethanol and isopropyl alcohol were less hydrated than 1,2-propanediol. In addition, short chain alcohols were probably mostly located within the interfacial film interacting with surfactant more strongly than the other two cosurfactants. This made them less available for hydrogen bonding with water molecules. Hence, mobility of water phase was higher, resulting in higher conductance as well.

Similar to the drug influence on pH, electrical conductivity values were also strongly affected by SN incorporation, which was also explained with the fact that nitrate anions increased the conductance by passing through water channels.

All selected MEs had low viscosity values (8.96-48.79 mPas) and characterized with Newton flow behavior (Figure 4a), which is the most common flow type for ME systems. According to the obtained low viscosity values together with polarization microscopy and AFM results, the existence of liquid crystalline structures was excluded. Among the tested formulations, P80

based ME had the highest value of apparent viscosity (48.79 ± 1.17). Having in mind that this sample had the same concentration of all ingredients as the ME-EVT formulation, one can conclude that the surfactant type and its structure affected rheology of the investigated ME systems. Namely, the surfactant having lower molecular weight (i.e. EV with Mr of 301.34) produced lower viscosity than P80 characterized with Mr 524.6. In addition, due to the larger number of the very hydrophilic polyoxyethylene head groups in its structure, P80 probably interacted *via* hydrogen bonds with water molecules more strongly, which reflected on the sample's viscosity. This observation coincides well with the lower conductivity values obtained for C90/P80/Transcutol® P/water system due to the more pronounced restriction of water mobility. In parallel with this trend, viscosity of quantitatively the same EV based formulations increased with increasing molecular weight of cosurfactants (ethanol < isopropyl alcohol < Transcutol® P) and was was in a range of 8.96 to 18.84 mPas. Apparently the propylene glycol based sample did not obey this relation. However, it should be noticed that ME-EVPG sample had less water and larger amount of other components (i.e. S-CoS and oil) than the other samples based on the same surfactant, which was determinant factor influencing its viscosity (32.63 ± 0.94 mPas). Also, 1,2-propanediol has an additional hydroxyl group in contrast to ethanol and isopropyl alcohol, thus an increase in the degree of hydration and higher viscosity may be expected.

Although the addition of SN did not alter MEs' flow behavior, the viscosity of drug-loaded samples was higher than of placebo MEs (11.90-51.01 mPas), suggesting that the drug influenced the microstructure of the investigated samples in a way that the droplet size increased or higher degree of S-CoS hydration was achieved. However, the change of viscosity was not of statistical importance. According to the increase of viscosity caused by the presence of the drug,

as well as the composition of selected samples (Table 2), solubility of SN in ME constituents [16] and logP value of the drug (6.2), the major fraction of the drug was probably partitioned between the oil phase and the less polar part of the interface.

Finally, with the intention to shed light on the interfacial properties of the S-CoS monolayer of MEs in the absence and the presence of the drug and thus to confirm our assumptions about the locus for drug solubilization, we further employed EPR spectroscopy. The spin-labeled amphiphilic fatty acid-5-DSA was used as a spin probe. This interface-located fatty acid spin probe gives EPR spectra reflecting the rigidity/flexibility of its environment from the depth of the membrane where the doxyl-ring of the 5-DSA is located. As a result, (i) alterations caused in the membrane in the presence of different types of surfactants/co-surfactants and (ii) the localization of the drug in the ME systems, were evaluated. In the case of 5- DSA the doxyl group is located closer to the polar head of the amphiphilic fatty acid and consequently closer to the S-CoS polar heads. However, it should be highlighted that EPR spectra of 5-DSA (pKa = 7.45) is pH dependent and the knowledge of sample's pH is strongly required for spectra's analysis [21].

The obtained results are presented in Figure 4b and Table 3. The investigated systems composed of C90/EV/cosurfactant/water showed distinct interfacial properties as expected. In the case of ME-EVPG system, the remarkable increase in the τ_R value could be due to the nature of 1,2-propanediol which restricts the rotational movement of the spin probe [39]. The observed decrease of the spin probe's mobility could be also explained by the reduction of the water content of the system, drastically affecting the microenvironment. In addition, ME-EVPG system contains higher quantity of oil and S-CoS mixture (Table 1) and has higher viscosity as well inducing bigger restriction to the probe movement. The presence of propylene glycol and the

decrease of water content also affected the order parameter values indicating the passing from a rather flexible packing of membrane to a more ordered state. The 5% w/w decrement of the water content also reflects on the value of the α_0' which was also reduced and indicates a less polar environment.

On the contrary, very low τ_R values were recorded for the MEs which are composed of C90, EV, cosurfactant and 30% of water. In this case not only τ_R values were decreased but also the order parameters were decreased from 0.17±0.02 to 0.11±0.01. When short chain alcohols were used as cosurfactants, the mobility of the spin probe was clearly affected with a characteristic alteration in the experimental spectrum where the peaks were narrower than those on ME-EVPG and ME-EVT systems (Figure 4b). This was a consequence of a more "free" movement of the spin probe when alcohols are present in the MEs creating a more polar and less strict environment for the mobility of the spin probe. Furthermore, the *S* parameter is also affected with a less rigid surfactant monolayer as observed in ME-EVI and ME-EVE systems. Therefore, the EPR studies were in consistence with phase behavior studies demonstrating a more flexible interfacial film for systems based on alcohols, which allowed the incorporation of larger amount of water.

Analyzing the influence of different surfactants on interfacial film properties, the higher τ_R value obtained for ME-P80T (Table 3) was probably due to the higher viscosity of P80 as compared to EV and the consequent difficulty of the paramagnetic nitroxide ring to rotate in the membrane. Therefore, the replacement of EV with another ethoxylated surfactant clearly shows that the rigidity of the membrane (parameter *S*), in the depth where the paramagnetic ring of the spin probe is located, was also affected since an increase from 0.15±0.01 to 0.16±0.03 was observed. However, the significant difference of pH values of ME-EVT and ME-P80T should not be

neglected as it could cause changes of the experimental EPR spectra. Namely, at higher pH (7.47) some of 5-DSA molecules (pKa = 7.45) might be ionized and thus located closer to the hydrophilic head groups of the surfactants. Contrary, in ME-P80T sample (pH = 4.42) only the unionized form of 5-DSA is expected. In this case the position of the doxyl group is among the hydrophobic tails of the surfactants, providing information only of this specific microenvironment.

EPR measurements of the five systems in the presence of SN were undertaken in order to obtain information about the possible drug effect on the interface of the formulations (Table 3). As shown in Table 3, for the 3 out of 5 systems (i.e. ME-EVT, ME-EVI and ME-EVE) the order parameter *S* and the rotational correlation time τ_R were not affected in the presence of SN, within the experimental error, meaning that the membrane rigidity remains unaltered after the incorporation of the drug. This is also corroborated with the fact that SN solubilization did not decrease formulations' micropolarity, which was anticipated from highly lipophilic character of SN. It has to be underlined that the part of the membrane that is examined with the use of 5-DSA is the part closer to the polar head of the spin probe's paramagnetic ring. Hence, it can be concluded from the above findings that SN is embedded within the oil. However, it cannot be excluded that the drug was also distributed among hydrophobic tails of the S-CoS, at least partially. In contrast to this, in the systems ME-P80T and ME-EVPG the incorporation of the drug seems to impose important restrictions on the mobility of the spin probe. In both cases, τ_R and S values appeared to be remarkably increased indicating drug's participation in the less polar membrane of the formulations. In the ME-EVPG system the increase in the S-CoS and oil content made the solubilization of the SN easier (Table 1). It seems that SN modified the interfacial film structure to a more ordered organization around the nitroxide group, enabling the

5-DSA probe to insert deeply among the hydrophobic surfactant tails, where the movement is less restricted. On the other hand, isotropic hyperfine splitting constants (α_0') did not change meaning that the recognizable environmental polarity of the paramagnetic moiety of 5-DSA is the same in the absence and in the presence of SN in all systems.

To summarize, the EPR did not detect any significant change at the polar part of the interface of the tested MEs caused by SN solubilization. According to this, the lipophilic drug is mainly distributed in the oil phase. Also, it cannot be excluded that some SN molecules are embedded between hydrophobic tails of the interfacial film in the vicinity of the oil phase. Although without statistical importance, the solubilization of SN in ME-EVPG and ME-P80T samples affected the polar part of the respective S-CoS monolayers in a different manner than of other investigated MEs implying the drug presence at the membrane. Different hosting microstructure in the latter samples could affect biopharmaceutical properties of the drug carriers [33].

However, significantly distinct pH of placebo and drug loaded samples (Table 2) should be taken into consideration, as at the acid environment (SN-loaded MEs) the paramagnetic ring senses the hydrophobic surfactant tails. Under these conditions 5-DSA dominantly exists in the unionized form and might be shifted in the nonpolar part of the interface affecting the EPR spectra. Therefore, the conclusions about SN effects on the interfacial film are difficult to make and should be taken cautiously, especially for ME systems based on EV, since their pH values are remarkably altered after drug incorporation.

3.4. Stability study

During a year of storage there had no signs of any physical change of placebo and SN loaded formulations, i.e. opalescence, turbidity, phase separation, SN precipitation. This was somehow anticipated, bearing in mind that ME systems are characterized with thermodynamic stability.

However, other investigated properties were altered, i.e. pH values as well as electrical conductivity (Table 2). The slight pH decrement observed for all samples can be attributed to the presence of free fatty acids as products of gradual hydrolytic degradation of C90. Due to the greater number of hydrogen ions, the increase in electrical conductivity was intuitively expected and it occurred in placebo samples and drug loaded MEs as well.

During the storage of a year at the room temperature, the drug content in MEs did not significantly change (Figure 5), suggesting acceptable preliminary stability of samples. This result also confirms that the conductivity and pH changes were derived from C90's degradation.

3.5. In vitro *release of sertaconazole nitrate*

Given that *in vitro* release study can provide useful information on the influence of various factors involved in delivery of a drug into the skin, its therapeutic efficacy and indirectly its bioavailability [40], we investigated whether or not the differences in composition and overall microstructure of selected MEs reflected on their *in vitro* liberation properties. The assessment of potential of novel colloidal drug carriers (MEs) to improve SN delivery into the skin departments was carried out *in vitro* using vertical diffusion cells (i.e. Franz cells) equipped with synthetic membranes.

As presented in Figure 6 and Table 4, greater cumulative amount (μg/cm^2) of SN was released from all MEs in comparison to the referent commercial product. The corresponding transmembrane fluxes were also higher. The observed difference was not statistically significant

only in the case of ME-EVT sample ($p = 0.07$). The drug release profiles observed for the investigated MEs were similar to each other. SN release occurred according to the zero order kinetic described with a linear relationship between the cumulative amount of SN released per unit area and time. This kinetic model indicates constant, concentration-independent drug release. Hence, it may be considered as an advantage as the drug retention within the skin for prolonged period could be expected. Contrary, drug release from the reference cream, somehow expected, differed from MEs and fitted best to the Higuchi model, suggesting that the drug released by diffusion controlled by the vehicle, and also reflected that SN is, at least partly, suspended within the vehicle.

The released amounts of the drug from ME vehicles were generally low and after 8h of the experiment reached values of 12.24-18.53% of the applied drug amount (Table 4). Nevertheless, a concentration of the drug released at the end of the experiment was less than 30% of the total amount of the drug applied in the donor compartment. Hence, the drug diffusion back into donor compartment was avoided and a "30% rule" was fulfilled [41].

As can be seen from Table 4, the amount and rate of drug release highly depended on the formulation composition with ME-EVT sample producing lower release rates when comparing with other formulations. Further, when analyzing quantitatively same EV based systems with distinct cosurfactants, a release-enhancing effect of short chain alcohols was evident. However, the difference between the influence of ethanol and isopropyl alcohol was not statistically important. Correlating the drug release with physicochemical characteristics of the formulations, it appears that the differences in rheological behavior influenced SN liberation from the investigated formulations. Cumulative amount of drug released was remarkably higher from the samples with lower viscosity, which facilitated drug diffusion. Also, according to the EPR results

(Figure 4b, Table 3), the microenvironment of the interface of ME-EVE and ME-EVI was more polar and less ordered than of ME-EVT vehicle. As a result of such an environment, the migration of SN through the interface with looser packing occurred in an enhanced manner [33]. Also, the S-CoS monolayer of these MEs, especially its polar part, had lower solubilization capacity for highly lipophilic drug, resulting in higher thermodynamic activity of SN and thus higher drug release. This is in agreement with the capacity of formulations for drug solubilization (Table 1). Accordingly, as the solubility of the drug in EV based systems was higher, the release of SN was lower most likely due to higher thermodynamic activity of the drug. Similar behavior was noticed by Zvonar and coworkers [42]. Indeed, the drug release followed the rank order ME-EVE > ME-EVI > ME-EVPG > ME-EVT, while the saturation solubility for SN was totally opposite. Therefore, it can be deduced that in EV containing formulations SN release was inversely dependent on the solubilization capacity of the carriers.

On the other hand, the results produced with ME-EVPG formulation can be explained neither with rheological properties nor on the basis of the micropolarity and interface mobility of the samples. According to the lower water content, lower values of α_0', more ordered microstructure and higher viscosity of the propylene glycol based sample than of ME-EVT, lower drug release was expected. Surprisingly, the release of SN was slightly higher from ME-EVPG formulation. The explanation for this can be different locus for SN solubilization revealed by EPR, lower solubilization capacity for the drug and higher thermodynamic activity.

Finally, the type of surfactant also seemed to play an important role, since SN release from ME-P80T, differing from ME-EVT only in surfactant type, was significantly higher (Figure 6, Table 4) in comparison with not only with ME-EVT but also with all other MEs. Unexpectedly, ME-P80T sample had the highest viscosity and this result concerning SN release was not anticipated,

implying that rheological properties had no decisive role on drug liberation. However, the explanation for this phenomenon might also be the lower solubility of the drug in P80 based ME system (Table 1) as well as in its constituents [16]. Furthermore, SN increased the microviscosity and the order degree of the interfacial film of ME-P80T, hinting that the drug interacted to the certain extent with the polar part of S-CoS monolayer and increased the interactions between its constituents toward denser packing. This process could maybe induce the occurrence of droplet water-continuous structure which reflected positively on drug liberation. Namely, drug mobility is higher if the drug is located at the interface of o/w microemulsions [12].

Taking overall release results in parallel with the solubility results (Table 1), the characteristics of the formulations (Table 2) and EPR study results (Figure 4b, Table 3), it can be deduced that SN release was predominantly dependent on the solubility of the drug within the studied formulations and the localization of the drug within the MEs. Viscosity of the drug loaded samples and the amount of water in MEs also might contribute in the process of drug liberation. Due to considerably higher release of SN, for further *ex vivo* penetration and permeation investigations we chose ME-EVE, ME-EVI and ME-P80T samples.

In addition, the obtained *in vitro* drug release findings suggested that the choice of ME constituents should be made carefully. Namely, a usual way to select ME ingredients is primary based on drug solubility study in various oils and amphiphiles. Excipients with highest potential to solubilize the investigated drug are considered to be most appropriate. Interestingly, according to our study, not only broader single phase areas can be produced, but also higher drug release can be reached when constituents with lower solubilization capacity were employed for ME formulation.

3.6. Ex vivo *penetration and permeation assessment*

Considering that porcine skin is commonly regarded as suitable model to predict *in vivo* situation on human skin, penetration/permeation test was carried out on porcine ear skin and results for the investigated ME formulations are presented in Figure 7 and Table 5. Delivery of SN was assessed according to the SN content penetrated into the skin per surface area (μg/cm^2) after the experiment had finished. This parameter was also used as a measure of formulation dermal delivery efficacy. As can be noticed, incorporation of SN in MEs increased the drug skin delivery significantly, compared with the referent cream formulation, with dermal delivery enhancement ratios (ER_D) in a range of 2.66-4.25 (Table 5). The high drug loading capacity of MEs, skin hydration by MEs and formulation components acting as skin penetration enhancers can be the reasons for better skin delivery performances of MEs over Mycosert® [12, 14, 28].

Among the MEs tested, ME-EVE sample provided the highest amount of the drug retained in the skin, which made it superior over other two MEs (ER_D = 4.65). Unexpectedly, P80 based sample emerged as at least efficient regarding targeting the drug into the skin despite the liberation of SN from this ME was the highest. Since SN concentration was the same in all three MEs, concentration gradient of the drug could not be regarded as decisive factor for differences in drug penetration. Our former *in vivo* study [16] showed that ME-P80T and ME-EVT samples had satisfying preliminary safety profiles and did not induce skin barrier impairment. However, although without statistical importance, a slightly higher increase of eritema index values was observed for the sample based on EV as the main surfactant. Therefore, stronger EV's interaction with skin lipids might be suggested, reducing the *stratum corneum* barrier function and enhancing the diffusion of the drug into the skin. However, according to skin penetration results,

short chain alcohols most likely contribute significantly to this effect, due to their well established penetration enhancing properties [43, 44].

In agreement with the amounts of SN released from the MEs stabilized with ethanol and isopropyl alcohol, which were slightly different, the efficacy of ME-EVE for drug retention within the skin turned out to be insignificantly higher due to the high standard deviation of the results. Similar results suggesting more pronounced effect of MEs containing ethanol have been also reported by other authors [20, 28, 45] . However, due to the residual amount of water in ethanol (96% v/v), ME-EVE formulation probably contained more water than the other samples. Hence, the increased dermal hydration by ethanol based formulation and hence more pronounced opening of channels for drug transport may be expected [12, 20]. Anyway, the proposed mechanism should be confirmed with appropriate *in vivo* skin performances study of ME formulations.

Comparing the obtained skin penetration results with the release results (Table 4), interestingly the formulations were not ranked in the same manner. Indeed, in terms of skin penetration the rank was ME-EVE > ME-EVI > ME-P80T > Mycosert®, while the drug release was ranked as ME-P80T > ME-EVE > ME-EVI > Mycosert®. Accordingly, we can conclude that the dermal delivery of the drug was not dependent on drug release and was in contrast to the SN liberation from the MEs. In fact, as the release from ME systems was slower, the drug retention in the skin was higher, confirming the proposed prolonged action of SN after loading in MEs. Moreover, the rank of skin penetration was opposite to the rank of drug loading, which was ME-EVE < ME-EVI < ME-P80T. Therefore, the decreased SN skin retention of P80 based sample may be attributed to the different SN distribution, higher drug solubility and thus higher affinity for the vehicle than for the skin [46]. Furthermore, the presence of components acting as skin

penetration enhancers contributed to SN skin penetration. It seems that short chain alcohols in combination with EV had more pronounced influence when compared with Transcutol® P and P80. Although Transcutol® P is considered to have an intrinsic enhancing effect *per se* [47], it has already shown that its power was lower than the efficacy of aforementioned alcohols [43]. Namely, short chain alcohols are known to improve the flux of MEs by altering the system's hydro/lipophilicity. Furthermore, due to penetration of cosurfactant in surfactant monolayer the interfacial film is getting more fluid. Similarly, the presence of alcohol affects the rotational freedom of skin lipid acyl chains leading to the fluidization of the intercellular lipid matrix [44]. Thus, beside from the influence on drug solubility in the vehicle, ethanol also alters the structure of the biomembrane by lipid extraction and its fluidization resulting in an increased permeability of the drug increases [29]. Indeed, EPR study revealed that the interface consisting of EV and short chain alcohols was more fluid and thus more fluctuating. This could enhance the interactions of ME-EVE and ME-EVI formulations with the skin. In addition, a possible explanation for the observed findings may be the supersaturation process and the increase of SN thermodynamic activity as a consequence. This occurs if a formulation contains any volatile constituents, which is the case with ME-EVE and ME-EVI samples. However, since occlusive conditions were set up during the entire permeation experiment, the evaporation was prevented and its impact was hence negligible.

Considering the permeation of SN through the skin, it should be emphasized that no SN was detected in receptor fluid under the experimental settings used. Accordingly, the entrance of the drug to systemic circulation is prevented, providing the avoidance of the systemic adverse reactions and, hence, targeted drug dermal delivery [1].

Taking together the overall results of this study, in spite of containing different cosurfactants, a superiority of EV based formulations for SN dermal delivery over the sample containing P80 as the main surfactant could be suggested. Regarding the influence of different cosurfactants, a higher penetration efficacy could be ascribed to the sample costabilized with ethanol, reproducing findings already reported [20, 28, 45]. When it comes to prediction of formulations' ability to deliver a drug in/across the skin, our results showed that physicochemical and biopharmaceutical characteristics can sometimes be misleading. The conducted permeation/penetration study underlined the necessity of comprehensive characterization of novel vehicles (such as MEs) for dermal drug delivery, which should include an adequate skin penetration/permeation test.

3.7. In vitro *antifungal activity*

The antifungal efficacy of the developed ME formulations, i.e. ME-EVE, ME-EVI and ME-P80T, was assessed and compared with commercially available drug product (Mycosert® cream) as a positive control and physiological saline buffer as a negative control. Figure 8 clearly illustrates the fungal growth and ability of each tested formulation to inhibit it. The study revealed that all of the tested samples were significantly more effective in inhibiting the fungus growth than the commercial cream (Figure 8, Table 5). The average zones of inhibition, indicating the antifungal efficacy of drug encapsulated in the MEs, were presented in Table 5. The microbiological studies were observed not to be synchronous with the *ex vivo* permeation studies. To be more precise, the most effective formulation turned to be the ME-P80T, having the mean zone of inhibition against *Candida albicans* 48.0 ± 2.65 mm, followed by ME-EVI and ME-EVE. The higher antifungal efficacy of P80 based sample can possibly compensate its lower

skin penetration ability. Therefore, besides from ME-EVE and ME-EVI formulations, ME-P80T could be also further developed as a promising carrier for targeted dermal delivery of SN.

4. Conclusion

The present study demonstrated that Emanon EV-E as a poorly explored surfactant for pharmaceutical preparations can be successfully employed for formulation of prospective colloidal drug carries for dermal drug delivery such as MEs. Stable systems are producible in combination with different cosurfactants (i.e. Transcutol® P, ethanol, isopropyl alcohol, propylene glycol) and over wide range of components' content. ~~Comprehensive physicochemical characterization using electrical conductivity measurements, DSC, AFM and EPR studies was carried out in order to investigate the possibility of formation systems with different inner microstructures.~~ MEs having (inverted) bicontinuous structure had shown to be appropriate for solubilization of the antifungal drug SN. Despite the incorporation of SN in the selected ME vehicles induced pH decrease accompanied by the increase of electrical conductivity and apparent viscosity~~. However, in spite of these alternations~~, the MEs' properties remained acceptable for skin application. Also, EPR study ~~proved that introduction of the drug in ME systems did not significantly influenced the polar part of the water-oil interface,~~ suggested the oil phase and the part of the interface closer to oil phase as the most important locus for SN solubilization. However, the interface of ME-P80T and ME-EVPG formulations was less polar and thus more capable to accommodate lipophilic SN. The stability study revealed certain changes of pH and conductivity, whereas the drug content was found to be insignificantly altered. Beside from having adequate physicochemical characteristics and preliminary stability, the developed MEs had superior drug release properties over commercial drug product. The drug retention within the porcine ear skin samples was higher from MEs as well, especially ~~*Ex vivo*~~

~~penetration/permeation study results highlighted the favorable performances of~~ the samples based on short chain alcohols ~~as compared with the formulation obtained with commonly used surfactant polysorbate 80, which produced the fastest SN liberation~~. Finally, ME-EVE, ME-EVI and ME-P80T proved to be more effective in inhibition of fungal growth than the tested commercial formulation. Therefore, ~~due to the high SN penetration into the skin and pronounced antifungal activity,~~ the chosen MEs represent promising vehicles for dermal delivery of SN in treatment of cutaneous fungal infections. However, in order to confirm the potential of MEs to deliver the drug into the infectious skin, further *in vivo* study of their effectiveness in animal or/and human models are strongly required.

Acknowledgment

The authors would like to acknowledge the financial support from the Ministry of Education, Science and Technological Development, Republic of Serbia, through the Project TR34031. The authors are grateful to Kao Chemicals Europe for their kind donation of Emanon EV-E and Gattefosse SAS for free samples of Capryol™ 90 and Transcutol® P.

References

[1] S. Güngör, M.S. Erdal, B. Aksu, New Formulation Strategies in Topical Antifungal Therapy, JCDSA, 03 (2013) 56-65.

[2] S. Heuschkel, A. Goebel, R.H. Neubert, Microemulsions--modern colloidal carrier for dermal and transdermal drug delivery, J Pharm Sci, 97 (2008) 603-631.

[3] J.D. Croxtall, G.L. Plosker, Sertaconazole: a review of its use in the management of superficial mycoses in dermatology and gynaecology, Drugs, 69 (2009) 339-359.

[4] M.M. Abdellatif, I.A. Khalil, M.A.F. Khalil, Sertaconazole nitrate loaded nanovesicular systems for targeting skin fungal infection: In-vitro, ex-vivo and in-vivo evaluation, Int J Pharm, 527 (2017) 1-11.

[5] E. Lopez-Montero, J.-F. Rosa dos Santos, J.J. Torres-Labandeira, A. Concheiro, C. Alvarez-Lorenzo, Sertaconazole-Loaded Cyclodextrin - Polysaccharide Hydrogels as Antifungal Devices, The Open Drug Delivery Journal, 3 (2009) 1-9.

[6] S.K. Mandlik, S.S. Siras, K.R. Birajdar, Optimization and characterization of sertaconazole nitrate flexisomes embedded in hydrogel for improved antifungal activity, J Liposome Res, (2017) 1-11.

[7] S.A.A. Radwan, A.N. ElMeshad, R.A. Shoukri, Microemulsion loaded hydrogel as a promising vehicle for dermal delivery of the antifungal sertaconazole: design, optimization and ex vivo evaluation, Drug Dev Ind Pharm, 43 (2017) 1351-1365.

[8] S. Sahoo, N.R. Pani, S.K. Sahoo, Microemulsion based topical hydrogel of sertaconazole: formulation, characterization and evaluation, Colloids Surf B, 120 (2014) 193-199.

[9] S. Sahoo, N.R. Pani, S.K. Sahoo, Effect of microemulsion in topical sertaconazole hydrogel: in vitro and in vivo study, Drug Deliv, 23 (2016) 338-345.

[10] G. Soliman, M. Attia, R. Mohamed, Poly(Ethylene Glycol)-block-Poly(ε-Caprolactone) Nanomicelles for the Solubilization and Enhancement of Antifungal Activity of Sertaconazole, Curr Drug Deliv, 11 (2014) 753-762.

[11] J. Zhang, B. Michniak-Kohn, Investigation of microemulsion microstructures and their relationship to transdermal permeation of model drugs: ketoprofen, lidocaine, and caffeine, Int J Pharm, 421 (2011) 34-44.

[12] J. Zhang, B.B. Michniak-Kohn, Investigation of microemulsion and microemulsion gel formulations for dermal delivery of clotrimazole, Int J Pharm, 536 (2017) 345-352.

[13] L.B. Lopes, Overcoming the cutaneous barrier with microemulsions, Pharmaceutics, 6 (2014) 52-77.

[14] R.M. Hathout, T.J. Woodman, S. Mansour, N.D. Mortada, A.S. Geneidi, R.H. Guy, Microemulsion formulations for the transdermal delivery of testosterone, Eur J Pharm Sci, 40 (2010) 188-196.

[15] M.J. Lawrence, G.D. Rees, Microemulsion-based media as novel drug delivery systems, Adv Drug Deliv Rev, 45 (2000) 89-121.

[16] N.Z. Bubic Pajic, M.N. Todosijevic, G.M. Vuleta, N.D. Cekic, V.D. Dobricic, S.R. Vucen, B.R. Calija, M.Z. Lukic, T.M. Ilic, S.D. Savic, Alkyl polyglucoside vs. ethoxylated surfactant-based microemulsions as vehicles for two poorly water-soluble drugs: physicochemical characterization and in vivo skin performance, Acta Pharm, 67 (2017) 415-439.

[17] M.N. Todosijevic, M.M. Savic, B.B. Batinic, B.D. Markovic, M. Gasperlin, D.V. Randelovic, M.Z. Lukic, S.D. Savic, Biocompatible microemulsions of a model NSAID for skin delivery: A decisive role of surfactants in skin penetration/irritation profiles and pharmacokinetic performance, Int J Pharm, 496 (2015) 931-941.

[18] M. Fanun, W.S. Al-Diyn, Electrical conductivity and self diffusion-NMR studies of the system: Water/sucrose laurate/ethoxylated mono-di-glyceride/isopropylmyristate, Colloids Surf A, 277 (2006) 83-89.

[19] A.S. Narang, D. Delmarre, D. Gao, Stable drug encapsulation in micelles and microemulsions, Int J Pharm, 345 (2007) 9-25.

[20] V. Savic, M. Todosijevic, T. Ilic, M. Lukic, E. Mitsou, V. Papadimitriou, S. Avramiotis, B. Markovic, N. Cekic, S. Savic, Tacrolimus loaded biocompatible lecithin-based microemulsions with improved skin penetration: Structure characterization and in vitro/in vivo performances, Int J Pharm, 529 (2017) 491-505.

[21] M. Fanun, V. Papadimitriou, A. Xenakis, Characterization of cephalexin loaded nonionic microemulsions, J Colloid Interface Sci, 361 (2011) 115-121.

[22] L.J. Berliner, Spin Labeling : Theory and Applications., Academic Press, 1976.

[23] J.P. Klare, H.J. Steinhoff, Spin labeling EPR, Photosynth Res, 102 (2009) 377-390.

[24] USP37-NF32, 2014. Chapter 1724: Semisolid drug products—performance tests, The United States Pharmacopeia 37-The National Formulary 32, United States Pharmacopoeial Convention, Rockville, MD 20852, 2014.

[25] E.A. Bseiso, M. Nasr, O.A. Sammour, N.A. Abd El Gawad, Novel nail penetration enhancer containing vesicles "nPEVs" for treatment of onychomycosis, Drug Deliv, 23 (2016) 2813-2819.

[26] P. Szumala, Structure of Microemulsion Formulated with Monoacylglycerols in the Presence of Polyols and Ethanol, J Surfactants Deterg, 18 (2015) 97-106.

[27] M.N. Todosijević, N.D. Cekić, M.M. Savić, M. Gašperlin, D.V. Ranđelović, S.D. Savić, Sucrose ester-based biocompatible microemulsions as vehicles for aceclofenac as a model drug: formulation approach using D-optimal mixture design, Colloid Polym Sci, 292 (2014) 3061-3076.

[28] G.M. El Maghraby, Transdermal delivery of hydrocortisone from eucalyptus oil microemulsion: effects of cosurfactants, Int J Pharm, 355 (2008) 285-292.

[29] N. Aggarwal, S. Goindi, R. Khurana, Formulation, characterization and evaluation of an optimized microemulsion formulation of griseofulvin for topical application, Colloids Surf B, 105 (2013) 158-166.

[30] R.G. Alany, T. Rades, S. Agatonovic-Kustrin, N.M. Davies, I.G. Tucker, Effects of alcohols and diols on the phase behaviour of quaternary systems, Int J Pharm, 196 (2000) 141-145.

[31] S.K. Mehta, G. Kaur, R. Mutneja, K.K. Bhasin, Solubilization, microstructure, and thermodynamics of fully dilutable U-type Brij microemulsion, J Colloid Interface Sci, 338 (2009) 542-549.

[32] G. Bhatia, Y. Zhou, A.K. Banga, Adapalene microemulsion for transfollicular drug delivery, J Pharm Sci, 102 (2013) 2622-2631.

[33] M. Cohen-Avrahami, A.I. Shames, M.F. Ottaviani, A. Aserin, N. Garti, On the correlation between the structure of lyotropic carriers and the delivery profiles of two common NSAIDs, Colloids Surf B, 122 (2014) 231-240.

[34] R.G. Alany, I.G. Tucker, N.M. Davies, T. Rades, Characterizing colloidal structures of pseudoternary phase diagrams formed by oil/water/amphiphile systems, Drug Dev Ind Pharm, 27 (2001) 31-38.

[35] S.K. Mehta, K. Bala, Volumetric and transport properties in microemulsions and the point of view of percolation theory, Phys Rev E, 51 (1995) 5732-5737.

[36] W. Naoui, M.A. Bolzinger, B. Fenet, J. Pelletier, J.P. Valour, R. Kalfat, Y. Chevalier, Microemulsion microstructure influences the skin delivery of an hydrophilic drug, Pharm Res, 28 (2011) 1683-1695.

[37] A.S. Goebel, U. Knie, C. Abels, J. Wohlrab, R.H. Neubert, Dermal targeting using colloidal carrier systems with linoleic acid, Eur J Pharm Biopharm, 75 (2010) 162-172.

[38] F. Podlogar, M. Gasperlin, M. Tomsic, A. Jamnik, M.B. Rogac, Structural characterisation of water-Tween 40/Imwitor 308-isopropyl myristate microemulsions using different experimental methods, Int J Pharm, 276 (2004) 115-128.

[39] V. Papadimitriou, S. Pispas, S. Syriou, A. Pournara, M. Zoumpanioti, T.G. Sotiroudis, A. Xenakis, Biocompatible microemulsions based on limonene: formulation, structure, and applications, Langmuir, 24 (2008) 3380-3386.

[40] V.P. Shah, A. Yacobi, F.S. Radulescu, D.S. Miron, M.E. Lane, A science based approach to topical drug classification system (TCS), Int J Pharm, 491 (2015) 21-25.

[41] S. Azarmi, W. Roa, R. Lobenberg, Current perspectives in dissolution testing of conventional and novel dosage forms, Int J Pharm, 328 (2007) 12-21.

[42] A. Zvonar, Rozman, B., Gasperlin, M., The Influence of Microstructure on Celecoxib Release from a Pharmaceutically Applicable System: Mygliol 812®/Labrasol®/Plurol Oleique®/Water Mixtures, Acta Chim Slov, 56 (2009) 131-138.

[43] S. Güngör, Bergisadi, N., Effect of penetration enhancers on in vitro percutaneous penetration of nimesulide through rat skin, Pharmazie, 59 (2004) 39-41.

[44] L. Roussel, Rawad, A., Gilbert, E., Pirot, F. and Haftek, M., Influence of Excipients on Two Elements of the Stratum Corneum Barrier: Intercellular Lipids and Epidermal Tight Junctions, in: N. Dragicevic, Maibach, H.I (Ed.) Percutaneous Penetration Enhancers Chemical Methods in Penetration Enhancement, Springer-Verlag GmbH, Berlin, 2015, pp. 69-90.

[45] C.H. Liu, F.Y. Chang, D.K. Hung, Terpene microemulsions for transdermal curcumin delivery: effects of terpenes and cosurfactants, Colloids Surf B, 82 (2011) 63-70.

[46] W. Zhu, A. Yu, W. Wang, R. Dong, J. Wu, G. Zhai, Formulation design of microemulsion for dermal delivery of penciclovir, Int J Pharm, 360 (2008) 184-190.

[47] E. Escribano, A.C. Calpena, J. Queralt, R. Obach, J. Doménech, Assessment of diclofenac permeation with different formulations: anti-inflammatory study of a selected formula, Eur J Pharm Sci, 19 (2003) 203-210.

Figure captions

Figure 1. a) Pseudo-ternary phase diagrams of systems C90/EV/cosurfactant/water, using as cosurfactants: Transcutol P, ethanol, isopropyl alcohol and propylene glycol, from the top to the bottom (marked regions represent ME systems, lines represent investigated dilution lines 8:2 with marked position of selected formulations) and b) electrical conductivity (mean ± SD, n = 3) of S-CoS/oil systems upon dilution with water (top) and the first derivative $d\log(K)/d\Phi_w$ as a function of the water volume fraction (Φ_w) (bottom)

Figure 2. DSC thermograms of investigated MEs in cooling mode

Figure 3. AFM 2D error signal and 3D topography images showing the structure of the

ME-EVI sample

Figure 4. a) The flow curves of selected placebo and drug loaded MEs and b) the EPR spectra of 5-DSA for placebo ME samples

Figure 5. Content of SN in selected MEs during one year of storage at room temperature

Figure 6. *In vitro* release of SN from investigated MEs determined across the synthetic dialysis membrane (mean ± SD, n = 6)

Figure 7. The total amount of SN penetrated from investigated MEs and the reference into the porcine ear skin *ex vivo*

Figure 8. *In vitro* antifungal activity of ME-EVE, ME-EVI and ME-P80T samples compared with the marketed Mycosert® cream

TABLES

Table 1. Composition of selected formulations and SN saturation solubility within the samples

Formulation	**ME-EVT**	**ME-EVE**	**ME-EVI**	**ME-EVPG**	**ME-P80T**
Capryol™ 90	14.0	14.0	14.0	15.0	14.0
Emanon EV-E	28.0	28.0	28.0	30.0	-
Polysorbate 80	-	-	-	-	28.0
Transcutol® P	28.0	-	-	-	28.0
Ethanol	-	28.0		-	-
Isopropyl alcohol	-	-	28.0	28.0	-
Propylene glycol	-	-	-	30.0	-
Water	30.0	30.0	30.0	25.0	30.0
Solubility of SN (mg/mL ± SD)	60.70 ± 6.98	28.05 ± 2.00	29.88 ± 2.36	47.80 ± 3.63	42.20 ± 0.03

Table 2. Physicochemical characteristics of investigated MEs 48 h after preparation and after a year of storage at room temperature

Formulation		48 h		1 year	
		pH	**Electrical conductivity (μS/cm)**	**pH**	**Electrical conductivity (μS/cm)**
ME-EVT	placebo	7.47 ± 0.12	62.50 ± 1.01	6.70 ± 0.01	76.63 ± 0.49
	SN loaded	4.39 ± 0.04	268.00 ± 2.00	4.27 ± 0.03	292.33 ± 0.58
ME-EVE	placebo	7.37 ± 0.09	94.63 ± 1.15	6.87 ± 0.02	116.47 ± 0.30
	SN loaded	4.65 ± 0.10	445.67 ± 4.04	4.52 ± 0.02	471.00 ± 1.73
ME-EVI	placebo	7.44 ± 0.03	71.50 ± 0.62	6.67 ± 0.06	81.047 ± 0.26
	SN loaded	4.62 ± 0.06	319.67 ± 2.31	4.38 ± 0.03	338.00± 1.00
ME-EVPG	placebo	7.38 ± 0.06	41.10 ± 0.62	6.88 ± 0.04	50.77 ± 0.06
	SN loaded	4.60 ± 0.08	182.00 ± 2.46	4.42 ± 0.03	204.33 ± 0.58
ME-P80T	placebo	4.42 ± 0.03	21.50 ± 1.10	4.28 ± 0.01	22.40 ± 0.10
	SN loaded	3.67 ± 0.11	242.33 ± 1.15	3.58 ± <0.01	278.33 ± 0.58

Table 3. Rotational correlation time (τ_R), order parameter (S) and isotropic hyperfine splitting constant (α_0') of 5-DSA in placebo and drug-loaded MEs

Formulation		5-DSA		
		τ_R (ns)	S	α_0'
ME-EVT	unloaded	2.99±0.06	0.15±0.01	14.06±0.03
	SN-loaded	2.81±0.05	0.15±<0.01	14.24±0.12
ME-EVE	unloaded	1.55±0.04	0.11±0.01	14.75±0.01
	SN-loaded	1.55±0.03	0.11±0.01	14.77±0.01
ME-EVI	unloaded	1.60±0.01	0.11±0.01	14.69±0.04
	SN-loaded	1.56±0.06	0.11±0.01	14.70±0.16
ME-EVPG	unloaded	3.83±0.08	0.17±0.02	13.64±0.13
	SN-loaded	4.26±0.19	0.21±0.03	13.65±0.17
ME-P80T	unloaded	3.14±0.01	0.16±0.03	13.85
	SN-loaded	4.22	0.20±0.01	-

Table 4. Release parameters of MEs and control formulation containing 2.0 % (*w/w*) of SN obtained through *in vitro* characterization across the dialysis membrane

Formulation	Transmembrane flux (µg/cm^2 h)	Q_{8h} (µg/cm^2)	SN released (%)	Kinetic model (r^2)
ME-EVT	163.97 ± 3.90	1218.39 ± 41.41	12.24 ± 0.42	zero (0.9927)
ME-EVE	217.87 ± 21.70	1562.44 ± 178.45	15.70 ± 1.79	zero (0.9937)
ME-EVI	206.64 ± 6.94	1524.44 ± 46.84	15.32 ± 0.47	zero (0.9967)
ME-EVPG	167.88 ± 2.28	1278.05 ± 38.21	12.84 ± 0.38	zero (0.9925)
ME-P80T	240.03 ± 8.42	1843.71 ± 78.45	18.53 ± 0.79	zero (0.9967)
Mycosert® cream	127.58 ± 4.75	1027.95 ± 10.42	10.33 ± 0.10	Higuchi (0.9942)

Table 5. Skin penetration study results and antimicrobial activity of MEs and control formulation containing 2.0 % (*w/w*) of SN

Formulation	SN retained in the skin (µg/cm^2)	Dermal enhancement ratio (ER_D)	Inhibition zone (mm)
ME-EVE	61.14 ± 15.17	4.25	40.0 ± 3.6
ME-EVI	43.22 ± 11.53	3.00	44.0 ± 0.87
ME-P80T	38.28 ± 7.01	2.66	48.0 ± 2.65
Mycosert® cream	14.39 ± 0.39	1.00	30.0 ± 0.5

Highlights

- Emanon EV-E was capable to produce microemulsion system over wide range of components
- SN affected physicochemical characteristics of systems
- Microemulsions enhanced *in vitro* drug release and dermal retention when compared with the control formulation
- Antifungal activity was greater in microemulsions
- Microemulsion formulations represent promising vehicles for topical application of SN

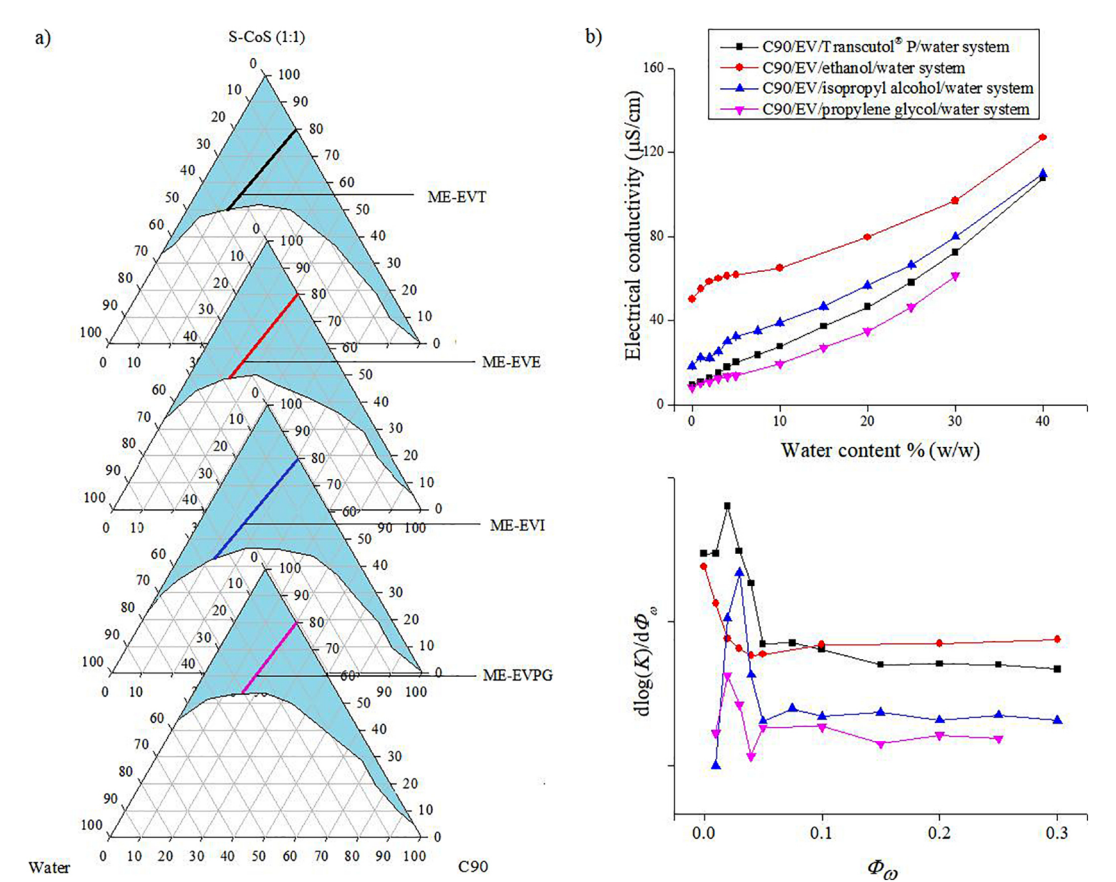
a)
S-CoS (1:1)
ME-EVT
ME-EVE
ME-EVI
ME-EVPG
Water
C90
b)
C90/EV/Transcutol® P/water system
C90/EV/ethanol/water system
C90/EV/isopropyl alcohol/water system
C90/EV/propylene glycol/water system
Electrical conductivity (μS/cm)
Water content % (w/w)
dlog(K)/dΦω
Φω

Figure 1

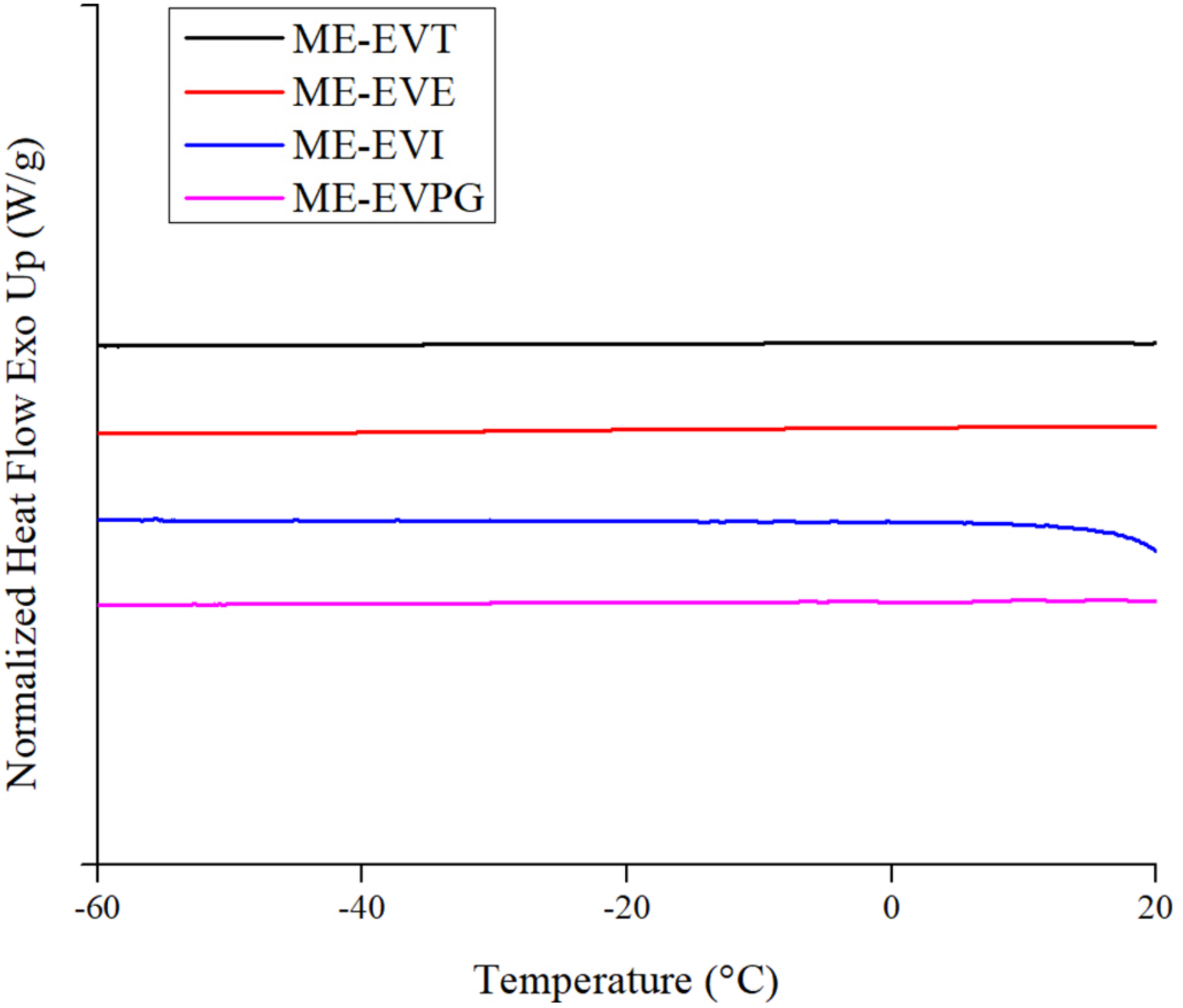
ME-EVT
ME-EVE
ME-EVI
ME-EVPG
Normalized Heat Flow Exo Up (W/g)
-60
-40
-20
0
20
Temperature (°C)

Figure 2

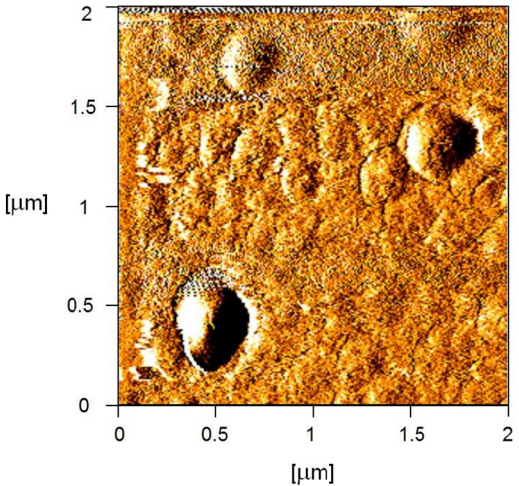

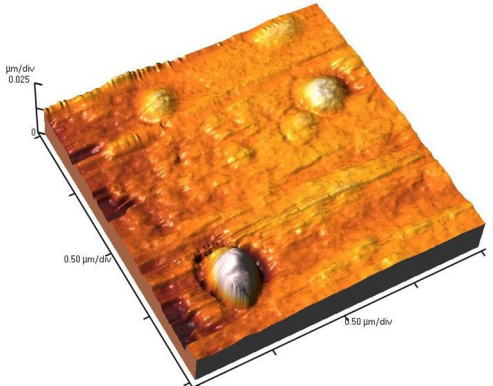

Figure 3

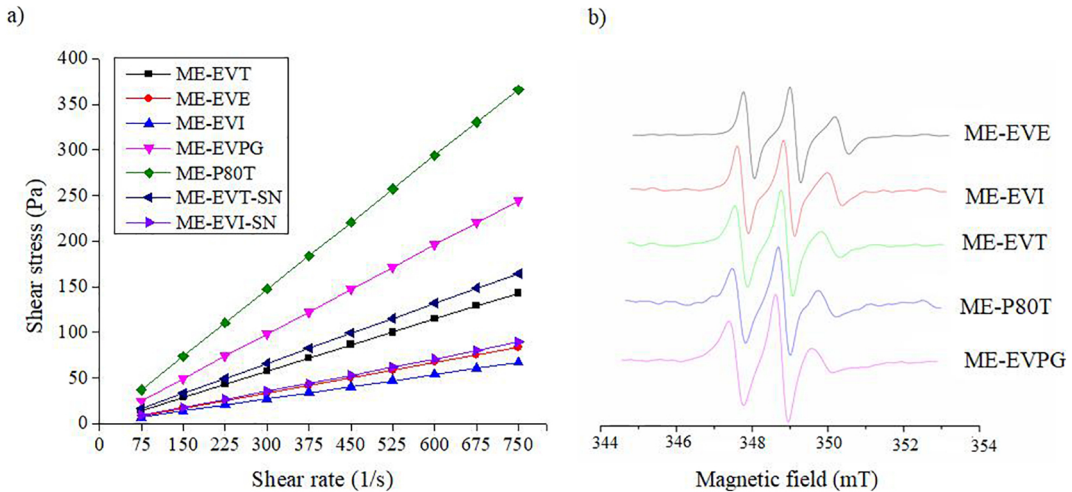
a)
b)
ME-EVT
ME-EVE
ME-EVI
ME-EVPG
ME-P80T
ME-EVT-SN
ME-EVI-SN
Shear stress (Pa)
Shear rate (1/s)
0
50
100
150
200
250
300
350
400
0
75
150
225
300
375
450
525
600
675
750
ME-EVE
ME-EVI
ME-EVT
ME-P80T
ME-EVPG
344
346
348
350
352
354
Magnetic field (mT)

Figure 4

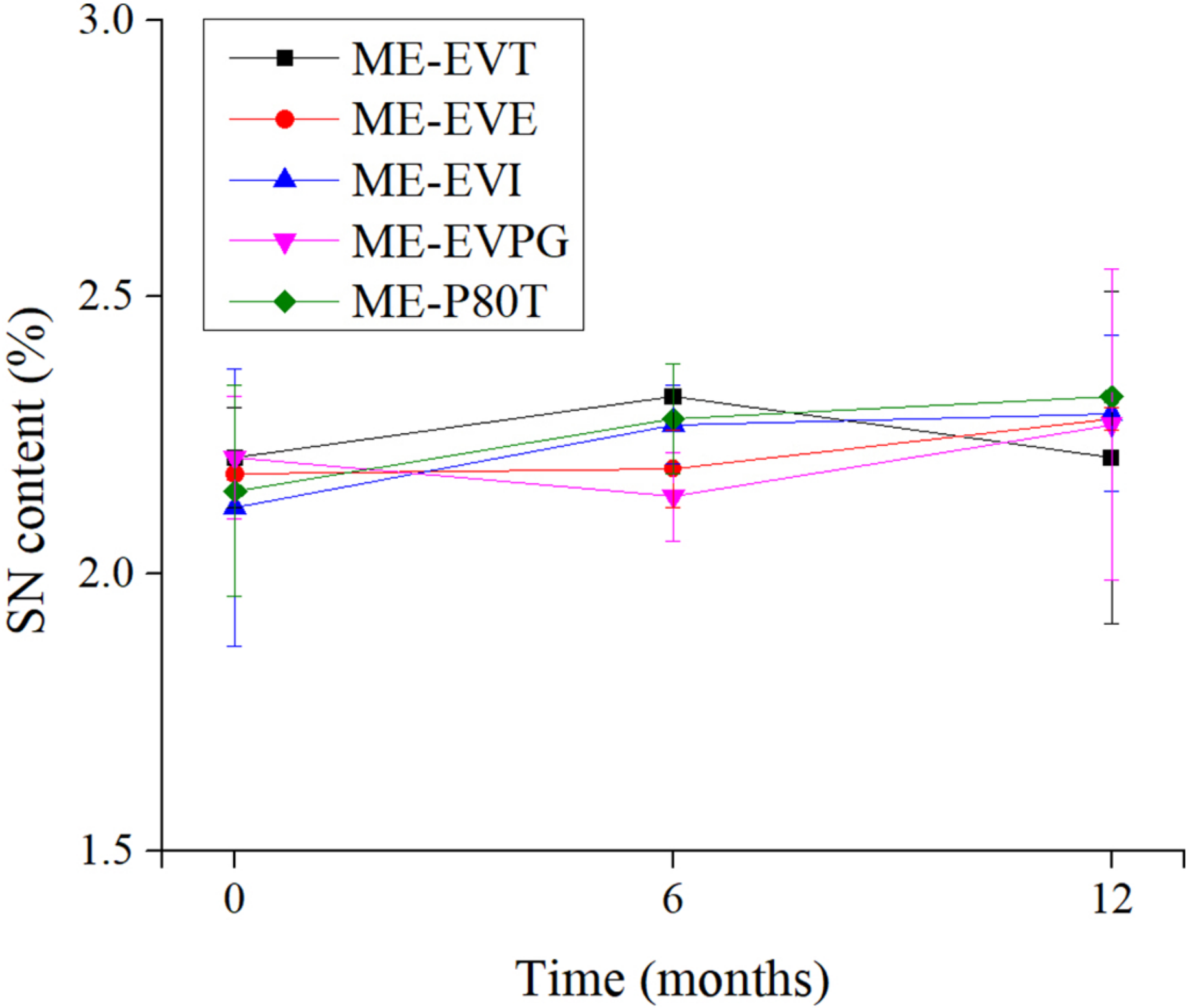
ME-EVT
ME-EVE
ME-EVI
ME-EVPG
ME-P80T
SN content (%)
3.0
2.5
2.0
1.5
0
6
12
Time (months)

Figure 5

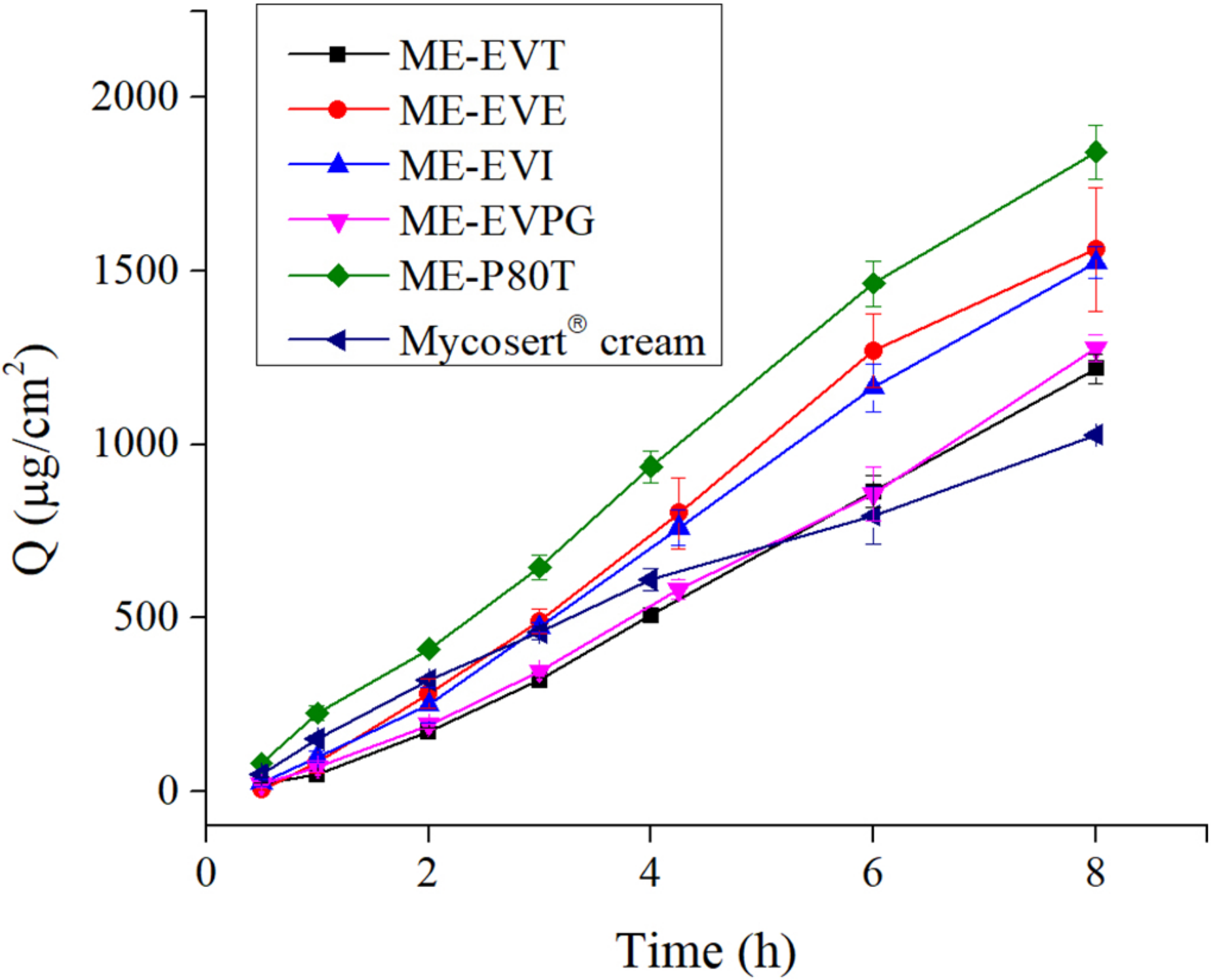
ME-EVT
ME-EVE
ME-EVI
ME-EVPG
ME-P80T
Mycosert® cream
Q (µg/cm²)
2000
1500
1000
500
0
0
2
4
6
8
Time (h)

Figure 6

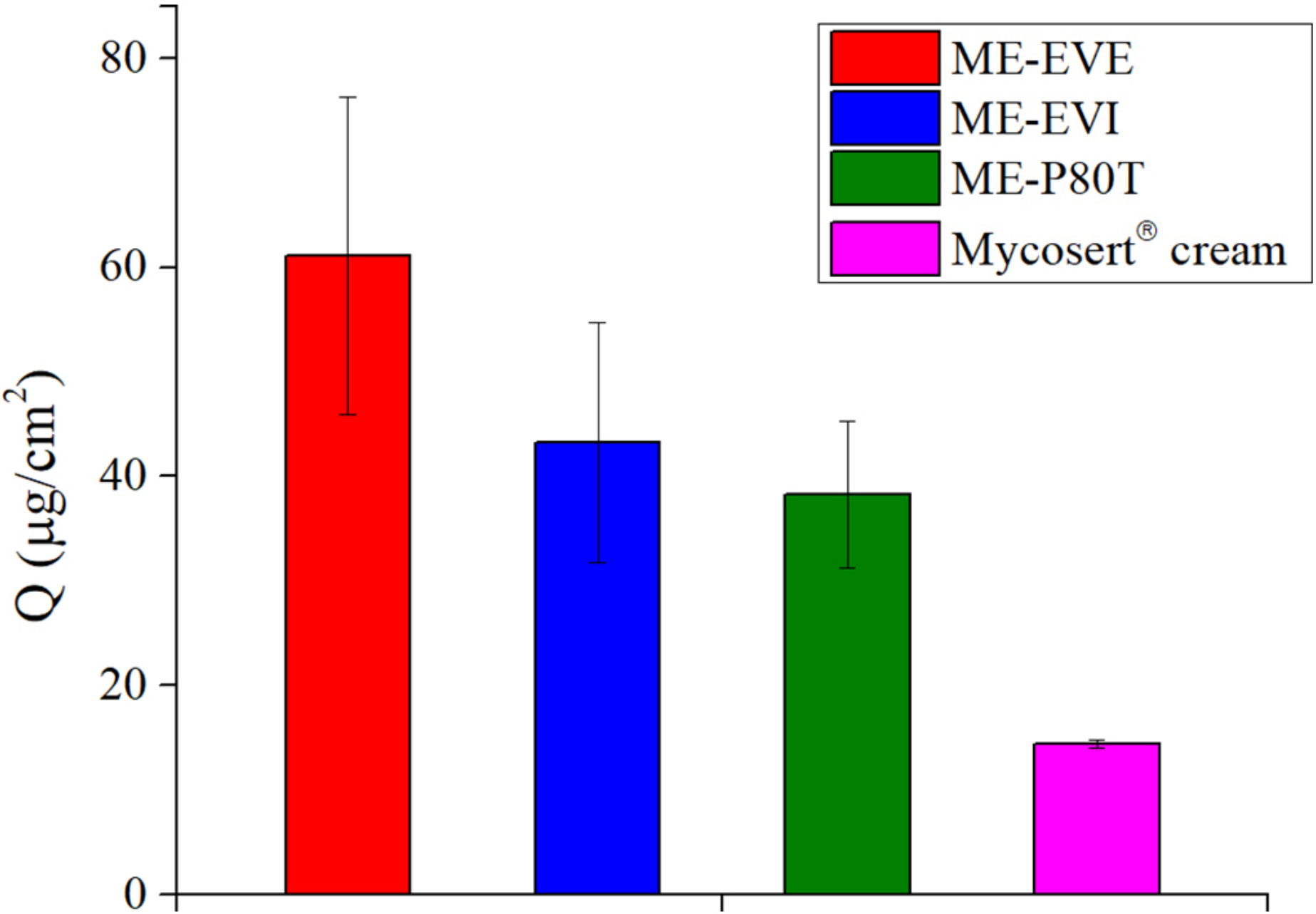

Figure 7

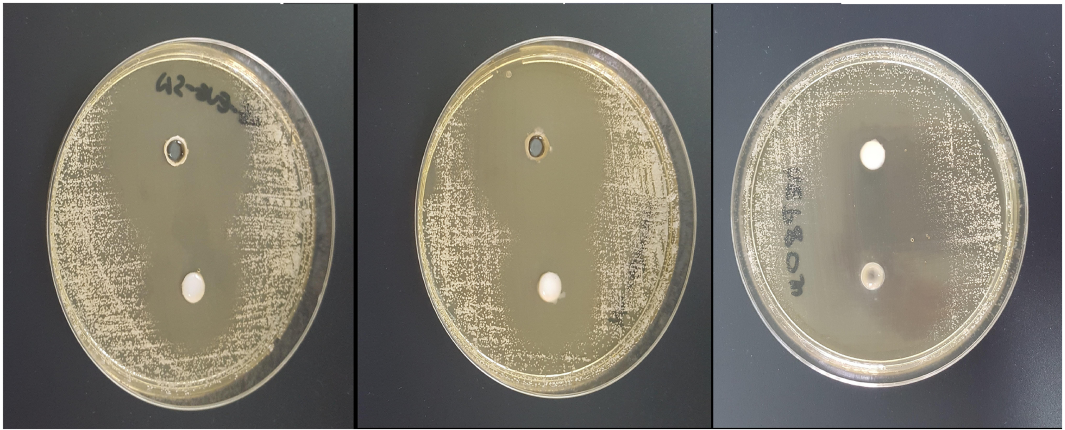

Figure 8